Marine Chemistry 157 (2013) 24–40

Contents lists available at ScienceDirect

Marine Chemistry

journal homepage: www.elsevier.com/locate/marchem

# Iron in land-fast sea ice of McMurdo Sound derived from sediment resuspension and wind-blown dust attributes to primary productivity in the Ross Sea, Antarctica

Jeroen de Jong [a,*], Véronique Schoemann [b], Nathalie Maricq [a], Nadine Mattielli [a], Patricia Langhorne [c], Timothy Haskell [d], Jean-Louis Tison [b]

[a] Laboratoire G-TIME, Géochimie-Traçage Isotopique, Mineral et Elémentaire CP 160/02, Département des Sciences de la Terre et de l'Environnement, Université Libre de Bruxelles, Avenue F.D. Roosevelt 50, B-1050 Brussels, Belgium
[b] Laboratoire de Glaciologie CP 160/03, Département des Sciences de la Terre et de l'Environnement, Université Libre de Bruxelles, Avenue F.D. Roosevelt 50, B-1050 Brussels, Belgium
[c] Sea Ice Group, Department of Physics, University of Otago, P.O. Box 56, Dunedin 9054, New Zealand
[d] Industrial Research Ltd., 69 Gracefield Road, P.O. Box 31310, Lower Hutt 5040, New Zealand

ARTICLE INFO

*Article history:*
Received 12 January 2013
Received in revised form 16 July 2013
Accepted 17 July 2013
Available online 3 August 2013

*Keywords:*
Iron
Sea ice
Sediments
Resuspension
Suspended particulate matter
Atmospheric particulates
Primary production

ABSTRACT

We present high-accuracy isotope dilution mass spectrometry data on dissolved Fe (DFe), total dissolvable Fe (TD-Fe) and refractory particulate Fe (REF-Fe) concentrations in snow, land-fast ice and under-ice seawater, sampled at six sites from 14 to 22 January 2003 in Erebus Bay, McMurdo Sound. We also report refractory particulate Fe/Al ratios to help identify Fe sources. Iron concentrations in land-fast ice and snow were two to three orders of magnitude higher than the underlying seawater. Seawater Fe increased in all fractions over the sampling period (8 days), likely caused by sediment resuspension induced by spring tides, which occur twice a month. We propose that entrainment of wind-blown material and sediment-derived Fe is the most important pathway for high Fe concentrations in land-fast ice in McMurdo Sound. Iron fluxes from the sediment were estimated and could fully account for the Fe inventory of the land-fast ice. Wind-blown lithogenic material in the snow on the land-fast ice makes up for 14–68% of the total Fe inventory of the sea ice. It does not appear to penetrate into the sea ice proper as snow-ice forming conditions were not present. The sources of these wind-blown particles are, in decreasing order of strength, the McMurdo Ice Shelf, the Dry Valleys, Ross Island and Erebus volcanic emissions. The data suggest that the usual spring breakup of sediment-laden land-fast ice to the Ross Sea may have a significant potential fertilizing effect on the waters of the Ross Sea Polynya. This is illustrated by the strong diminution of primary production in the Ross Sea Polynya due to the blockade of the annual sea ice breakout by the giant icebergs B-15 and C-19 during the austral summer of 2003.



## 1. Introduction

The surface of Antarctic sea ice varies seasonally between $3.8 \times 10^6$ km$^2$ (summer) and $19 \times 10^6$ km$^2$ (winter) (Comiso, 2003). As an ocean–atmosphere interface, sea ice has a considerable impact on the polar environment. Its influence ranges from the formation of polar deep water masses involved in the global thermohaline circulation, the global radiation budget via albedo effects on the lower atmosphere as well as via the heat and light distribution in the water column, to an important ecological role as provider of a stable habitat for diverse communities of (micro)-organisms (Garrison et al., 1986; Legendre et al., 1992).

The role that sea ice could play in the marine biogeochemical cycle of iron (Fe) has long been neglected due to the challenging sampling environment. Iron plays an essential role as micronutrient for phytoplankton growth in the regulation of the marine carbon pump (Boyd et al., 2007). The assessment of sea ice as a Fe fertilizing factor for the polar oceans is likely to have consequences for paleo-climatological reconstructions and the prediction of future climate change. A number of recent studies (Grotti et al., 2005; Lannuzel et al., 2007, 2008, 2010; van der Merwe et al., 2009, 2011a,2011b) have highlighted the capability of Antarctic sea ice to accumulate Fe, with observed dissolved and particulate Fe concentrations one to two orders of magnitude higher than the underlying seawater. The mechanism by which the Fe is accumulated is unclear to date, but may involve scavenging during sea ice formation of biogenic (Ackley and Sullivan, 1994) and lithogenic particles (Grotti et al., 2005; van der Merwe et al., 2011a), Fe sequestration by sea ice algae (Lannuzel et al., 2010) and accumulation of atmospheric dust on the ice (Sedwick et al., 2000; Fitzwater et al., 2000; Sedwick and DiTullio, 1997). During the seasonal melting of sea ice, this Fe is released in the surface waters (Lannuzel et al., 2008) and may be a triggering factor for phytoplankton blooms (Sedwick and DiTullio, 1997; Goffart et al.,

* Corresponding author. Tel.: +32 2 6502246.
*E-mail address:* jdejong@ulb.ac.be (J. de Jong).

0304-4203/$ – see front matter © 2013 Elsevier B.V. All rights reserved.
http://dx.doi.org/10.1016/j.marchem.2013.07.001

2000) at the retreating ice edge or in polynyas (Arrigo and van Dijken, 2003).

In this paper we will discuss results from a survey in January 2003 of Fe concentrations in snow, sea ice and seawater in Erebus Bay (McMurdo Sound). We hypothesize that land-fast ice from McMurdo Sound is an important vector of natural Fe fertilization of the Ross Sea, thanks to atmospherically (McMurdo Ice Shelf, Dry Valleys, Ross Island, Erebus volcano) and sedimentary (sea floor sediment resuspension and ice shelf basal debris) derived Fe.

## 2. Geological, hydrographical and glaciological setting

### 2.1. Geology

McMurdo Sound is a small marginal basin surrounded by the Transantarctic Mountains of Victoria Land to the west, the McMurdo Ice Shelf (MIS) to the south, Ross Island to the east and the Ross Sea to the north (Fig. 1A). Ross Island is the site of the most active volcano in Antarctica: Mount Erebus (Del Carlo et al., 2009) (Fig. 1A and B). The bulk of exposed lava flows on the Erebus volcano cone is distinctively phonolitic, contrasting with the surrounding areas on Ross Island forming the broad platform shield of the Mount Erebus edifice and consisting predominantly of basanitic lavas (Kyle, 1976). The volcanic bedrock to the south and the west of McMurdo Sound is also basanitic in nature (Kyle, 1976). Phonolitic and basanitic lavas exhibit characteristic Fe/Al ratios, which can be useful to trace sources of Fe, e.g., basanite median molar Fe/Al = 0.60 ± 0.03 (n = 91) (Table 1) and phonolite median molar Fe/Al = 0.18 ± 0.02 (n = 55) (Table 1).

Victoria Land is the scene of one of the world's most extreme deserts, the McMurdo Dry Valleys, a large 4000 km$^2$ ice-free area (Bockheim, 2002) with very low humidity and precipitation. High katabatic winds blow dust and gravel into the coastal zone (Ayling and McGowan, 2006) with intermediate molar Fe/Al compositions (median 0.41 ± 0.06, n = 269, Table 1).

On the MIS, glacial debris bands lie openly exposed on the ice shelf surface (Atkins and Dunbar, 2009; Dunbar et al., 2009), which with the prevailing southerly wind direction are subject to wind erosion and transport of wind-blown dust into McMurdo Sound. This wind-blown dust has a median Fe/Al of 0.45 ± 0.03 (n = 24) (Table 1).

### 2.2. Hydrography

The western shelf of McMurdo Sound has water depths of about 200 m, which slowly increases towards the east to 900 m depth nearshore of Ross Island, where the shelf slope is very steep (Fig. 1C). A cyclonic oceanic circulation pattern brings relatively warm and salty Antarctic Surface Water (AASW) from the Ross Sea along the west coast of Ross Island in southerly direction where it returns north along the coast of Victoria Land and by doing so entrains Ice Shelf Water (ISW) from underneath the MIS (Barry and Dayton, 1988).

### 2.3. Glaciology

Land-fast ice is formed in the Sound during winter, between late March and early December (Jeffries et al., 1993), and reaches an average

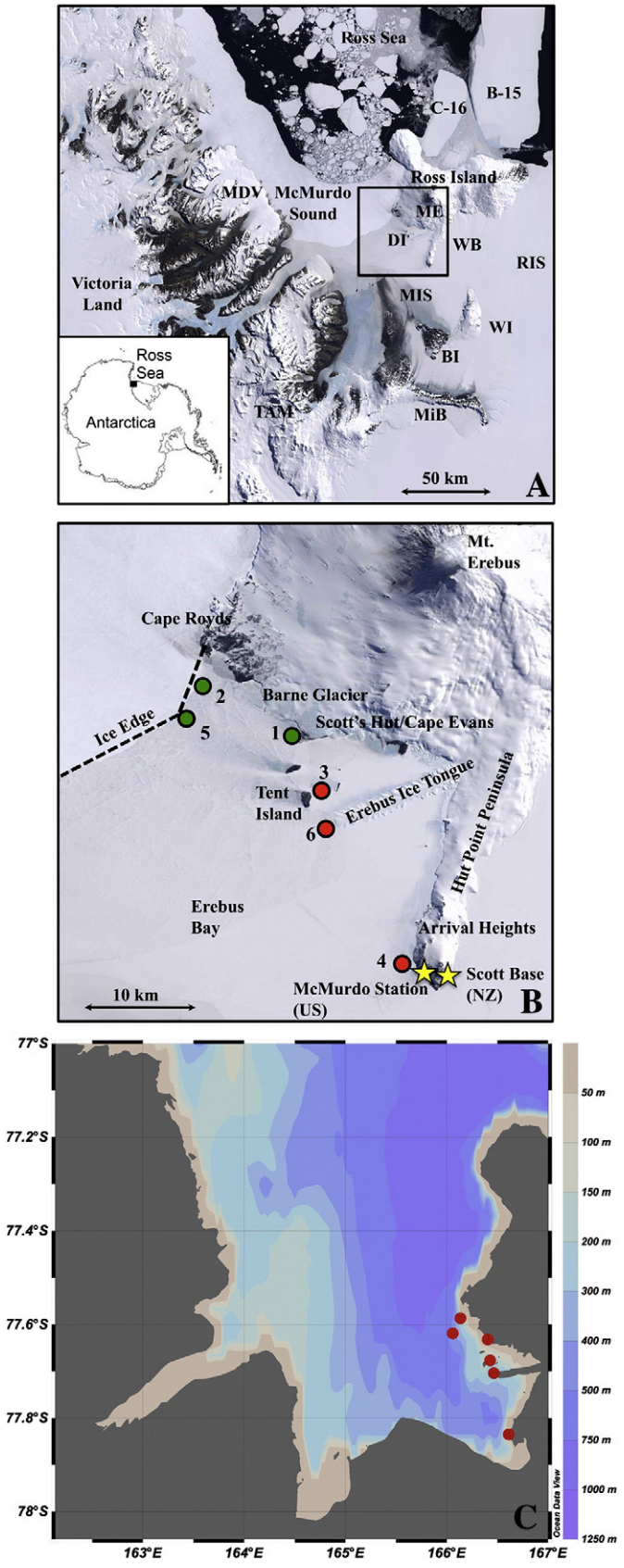


**Fig. 1.** (A) Composite of satellite images of Ross Island, McMurdo Sound and Victoria Land with geographic abbreviations: BI (Black Island), DI (Dellbridge Islands), MiB (Minna Bluff), MDV (McMurdo Dry Valleys), ME (Mount Erebus), MIS (McMurdo Ice Shelf), RIS (Ross Ice Shelf), TAM (Transantarctic Mountains), WB (Windless Bight), WI (White Island). Also indicated are giant iceberg B-15 and smaller iceberg C-16. Giant iceberg C-19 was further to the north (see Arrigo and van Dijken, 2003). (B) Blown up section of research area comprising Erebus Bay and western Ross Island with station positions. Green circles represent stations with first-year sea ice, while red circles are stations with multi-year sea ice. Satellite imagery (Terra-MODIS) is courtesy of NASA. (C) General bathymetry of McMurdo Sound, with the ice stations represented as red dots (see also B). Courtesy of Ocean Data View.

**Table 1**
Molar Fe/Al ratios in exposed lithogenic and marine materials from the McMurdo Sound area.

| Region | Material type | Median[a] | MAD[a] | n | References |
|---|---|---|---|---|---|
| South of Erebus Bay | Basanite rock | 0.59 | 0.03 | 58 | [b] |
| | Phonolite rock | 0.15 | 0.04 | 13 | |
| | Intermediate rock | 0.29 | 0.08 | 8 | |
| | Soil/wind-blown material | 0.45 | 0.03 | 24 | |
| | All | 0.54 | 0.08 | 103 | |
| East of Erebus Bay | Basanite rock | 0.59 | 0.06 | 12 | [c] |
| | Phonolite rock | 0.19 | 0.02 | 42 | |
| | Intermediate rock | 0.34 | 0.06 | 28 | |
| | Aerosol Erebus | 0.63 | 0.03 | 3 | |
| | All | 0.25 | 0.08 | 85 | |
| West of Erebus Bay | Basanite rock | 0.62 | 0.02 | 21 | [d] |
| | Phonolite rock | – | – | – | |
| | Intermediate rock | 0.26 | 0.04 | 11 | |
| | Soil/wind-blown material | 0.41 | 0.06 | 269 | |
| | All | 0.41 | 0.07 | 301 | |
| All data | Basanite rock | 0.60 | 0.03 | 91 | |
| All data | Phonolite rock | 0.18 | 0.02 | 55 | |
| | Marine sediment McMurdo Sound | 0.32 | 0.04 | 289 | [e] |
| This study: Erebus Bay | Snow | 0.38 | 0.05 | 4 | |
| | Sea ice Chl $a$ < 0.5 μg/L | 0.29 | 0.09 | 17 | |
| | Sea ice Chl $a$ > 0.5 μg/L | 0.51 | 0.11 | 11 | |
| | Under-ice seawater | 0.12 | 0.04 | 3 | |

[a] Median ± MAD: MAD is the median absolute deviation, meaning the median of the absolute deviations from the data's median (Hampel, 1974).
[b] Atkins and Dunbar (2009), Del Carlo et al. (2009), Cooper et al. (2007), Crockett (1998), and Kyle (1976).
[c] Kelly et al. (2008), Kyle et al. (1990), and Kyle (1976).
[d] Mahaney et al. (2009), Bull (2009), Williamson et al. (2007), Bertler et al. (2004), Sleewaegen et al. (2002), Bishop et al. (2001), and Kyle (1976).
[e] Damiani and Giorgetti (2008), Krissek and Kyle (2001), and Hieke Merlin et al. (1991).

thickness of 1.5 to 2 m (Atkins and Dunbar, 2009; Rémy et al., 2008). When the sea freezes, frazil ice forms as small needles, spicules or platelets (Eicken, 2003) that rise to the sea surface where it consolidates into granular ice. Frazil ice on its way to the surface scavenges suspended particulate matter (Ackley and Sullivan, 1994), such as algae, organic detritus and lithogenic sedimentary or terrestrial material. Columnar crystals form beneath this (Jeffries et al., 1993; Gow et al., 1998; Smith et al., 2001; Leonard et al., 2006), and are characteristic of sea ice growth in quiescent conditions. During this phase of ice formation, impurities such as sea salt are rejected from the crystalline matrix and become trapped in a network of brine pockets and brine channels. The interface between the sea ice and the underlying seawater is porous, and it is in this lowermost layer that growth of sea ice algae is mostly occurring. Near ice-shelves, platelet ice may be present at the base of the sea ice as a distinct feature of land-fast ice. Basal ice shelf melting produces ISW, which is colder and fresher than the surrounding seawater. Its higher buoyancy causes it to rise to the surface, during which it becomes supercooled and forms frazil ice (e.g., Smedsrud and Jenkins, 2004). Platelet ice is the name given to this ice when it is observed underneath sea ice. The formation of platelet ice in the sea ice cover has been linked to the time-history of the appearance of ice crystals in the supercooled water column (e.g., Leonard et al., 2006; Mahoney et al., 2011). Under these circumstances the ocean acts as a heat sink, contributing to the thickness of sea ice (e.g., Trodahl et al., 2000; Purdie et al., 2006). The observations of Leonard et al. (2006) and Purdie et al. (2006) were made between February and September 2003, immediately following those described here and in similar iceberg-affected conditions (Rémy et al., 2008).

In summer, melting of the sea ice by the incoming warmer Ross Sea water provokes the breakup of the ice cover by ocean swells and the ice floes are transported out into the Ross Sea. The period 2000–2003 was exceptional in that McMurdo Sound was partially blocked by the giant iceberg B-15. It perturbed the usual advection of AASW from the Ross Sea to the north (Robinson et al., 2010; Dinniman et al., 2007) and restricted the first-year spring breakout of sea ice. This led to the heaviest pack ice conditions ever registered in McMurdo Sound with an accumulation of land-fast ice to an average thickness of more than 3 m due to the formation of multi-year ice (Rémy et al., 2008). The combined perturbation by the giant icebergs B-15 and C-19 in 2003 also caused the late seasonal opening of the Terra Nova Bay and Ross Sea Polynyas (Dinniman et al., 2007). The unusual high sea ice cover in the Ross Sea led to a dramatic decrease of primary productivity with repercussions for higher trophic levels (Arrigo and van Dijken, 2003; Arrigo et al., 2002).

## 3. Material and methods

### 3.1. Sampling and sample processing

In January 2003, sea ice cores were extracted on six sites in Erebus Bay in southeastern McMurdo Sound (see Fig. 1B and Table 2 for a station overview). We largely followed the methods described in Lannuzel et al. (2006). We did not yet use an electro-polished core barrel (as in Lannuzel et al., 2006), but a Teflon coated stainless steel core barrel with a length of 1 m and a diameter of 7.5 cm. The drill was electrically driven with the power generator placed several tens of meters downwind of the sampling site. The trace metal ice core was drilled after drilling cores for other parameters, in order to decontaminate the core barrel. Cores were packed in multiple acid-cleaned plastic bags. Seawater samples were taken in 2 L LDPE bottles by pumping the water from 40 to 100 cm underneath the ice cover using a portable peristaltic pump (Masterflex E/S) with silicon pump tubing. Snow samples were taken immediately after arrival on the sampling site by scooping up snow with plastic ice scoops into 2 L LDPE bottles. All samples were stored deep-frozen until further processing at ULB. All plastic materials coming in contact with the samples were previously acid cleaned and copiously rinsed with ultrahigh purity (UHP) water from a Millipore Element water purification system. Prior to use, metallic sampling gear, such as the core barrel, decontamination chisel and ice saw were cleaned with methanol, rinsed with copious amounts of UHP water, dried with clean room tissue and kept in plastic bags. Personnel working on the sampling site were wearing Tyvek clean room apparel, nitrile gloves and plastic bags around boots.

For all of the Chlorophyll $a$ data from the same survey (Rémy et al., 2008) corresponding Fe samples were analyzed in a different ice core taken within a 1 m distance, parallel with the ice core for Chl $a$ analysis. For those stations where this led to less than six depths, additional depths were selected (station 3/194–210 cm, station 4/265–279 cm, station 5/164–175 cm, station 5/175–186 cm, station 6/186–200 cm). Slices of 10 to 14 cm thick were cut with a stainless steel hand saw, upon which each slice was decontaminated with a titanium chisel and placed in a large Savillex PFA pot with closure to melt. Snow and unfiltered seawater samples, which had been stored frozen, were thawed in their sample bottles. From the sea ice, snow and seawater samples, unfiltered and filtered splits of 250 mL were taken for determination of total dissolvable Fe (TD-Fe) and dissolved Fe (DFe), respectively.

Samples were filtered using polycarbonate filtration devices (Sartorius) with polycarbonate membrane filters (Nuclepore, 0.2 μm pore size, 47 mm diameter). Gentle vacuum (<0.5 bar) was applied with a Masterflex hand pump. The samples were acidified to pH 1.9 with 250 μL concentrated subboiled $HNO_3$ to 250 mL of sample.

### 3.2. Sample preparation and Fe analysis

Full details on sample preparation and Fe analysis can be found in de Jong et al. (2008). Briefly, TD-Fe and DFe in snow, ice melt and seawater were analyzed by isotope dilution multiple collector inductively coupled plasma mass spectrometry (ID-MC-ICP-MS) using a $^{54}Fe$ spike. In most cases 25 μL of a 500 μg/L $^{54}Fe$ was added (final concentration 4.4 nM $^{54}Fe$) to a volume of 50 mL of sample. In some cases, such as

**Table 2**
Station data. Air temperatures (24 h periods) monitored at Scott Base (NZ).

| Station # | | Locality | Latitude ° dec S | Longitude ° dec E | Sampling date dd-mm-yyyy | Water depth m | Distance to shore m | Air temp. max. °C | Air temp. min. °C | Air temp. avg. °C |
|---|---|---|---|---|---|---|---|---|---|---|
| 1 | First-year | Scott's Hut | −77.632 | 166.406 | 16-01-2003 | 50 | 180 | 1.6 | −5.4 | −1.9 |
| 2 | First-year | Barne Glacier | −77.587 | 166.136 | 17-01-2003 | 400 | 720 | 0.9 | −5.6 | −2.4 |
| 3 | Multi-year | Tent Island | −77.677 | 166.429 | 18-01-2003 | 190 | 240 | −3.7 | −7.4 | −5.6 |
| 4 | Multi-year | Arrival Heights | −77.835 | 166.611 | 14-01-2003 | 100 | 120 | −3.1 | −6.8 | −5.0 |
| 5 | First-year | Ice Edge | −77.619 | 166.060 | 22-01-2003 | 450 | 1320 | 2.8 | −1.6 | 0.6 |
| 6 | Multi-year | Erebus Ice Tongue | −77.704 | 166.465 | 19-01-2003 | 310 | 720 | −0.3 | −6.9 | −3.6 |

for unfiltered snow samples or bottom ice we deviated from this to prevent under- or overspiking, for instance by decreasing the sample volume or increasing the spiking volume. Sample preparation consisted of a pre-concentration step on micro-columns filled with NTA Superflow resin (Qiagen). Measurements were done at ULB using a Nu Plasma MC-ICP-MS (Nu Instruments, Wrexham, UK) operated in low resolution, and in dry plasma mode using an Aridus II desolvating sample inlet system (Cetac Technologies, Omaha, NE, USA). Dry plasma mode greatly reduces the formation of argon based polyatomic inferences (de Jong et al., 2008). Procedural blanks were obtained for the three analytical sessions during which the samples were extracted: 0.051 ± 0.027 (n = 2), 0.064 ± 0.010 nmol/L (n = 3) and 0.171 ± 0.044 nmol/L (n = 2). Simultaneous with the analytical work we analyzed SAFe reference seawater (Johnson et al., 2007) for quality control. Consensus values are as follows: Surface-1 (0.094 ± 0.008 nmol/L, 1 SD) and Deep-2 (0.923 ± 0.029 nmol/L, 1 SD). Our average values for Surface-1 (0.073 ± 0.013 nmol/L, 1 SD, n = 7) and Deep-2 (0.946 ± 0.032 nmol/L, 1 SD, n = 9) are in good agreement with the consensus values.

Total dissolvable Fe consists of the sum of DFe and a dilute nitric acid (0.014 mol/L, pH 1.9) dissolvable portion of the particulate Fe, with some refractory Fe possibly escaping dissolution and detection. To obtain total Fe concentrations (TOT-Fe), the refractory particulate Fe (REF-Fe) concentrations have been measured. This was determined by filtering (as described above) 100 mL of the unfiltered acidified samples that had been taken for TD-Fe. The filters were digested by following the method of de Jong et al. (2007) with a mixture of $HNO_3/H_2O_2$/HF (2000/500/250 μL) in Savillex screw cap beakers to which was added 50 μL of a 500 μg/L $^{54}Fe$ spike. They were heated for 24 h on a Teflon coated hotplate at 100 °C in a clean air chemical work station. Subsequently, the samples were dried down, and the residues were re-digested in $HNO_3/H_2O_2$ (2000/500 μL) to assure breakdown of organic matter. The samples were dried down again and re-dissolved in 0.05 M $HNO_3$ for analysis. Filter digestion blanks amounted to 8.3 ± 1.7 ng Fe (1 SD, n = 12), resulting in a detection limit (3 SD of the blank) of 5.1 ng. We chose to measure the filter digests without further purification to minimize the blank. To demonstrate the fitness for purpose of the acid-digestion method for biological and lithogenic sample types, we tested the reference materials IAEA-392 (green algae) and IAEA-405 (estuarine sediment) from the International Atomic Energy Agency as well as DC-75301 (offshore marine sediment) from the China National Analysis Centre. Results were as follows: IAEA-392 = 504 ± 3 μg/g (2 SD, n = 2, certified value IAEA-392: 497 ± 13 μg/g, recovery 101%), IAEA-405 = 3.80 ± 0.08% (2 SD, n = 2, certified value IAEA-405: 3.74 ± 0.07%, recovery 102%), DC-75301 = 3.59 ± 0.22% Fe (2 SD, n = 3, certified value DC-75301: 3.75 ± 0.16%, recovery 96%). The excellent agreement with the certified values demonstrates the absence of significant interference and completeness of the digestion.

To determine Fe/Al ratios, we measured REF-Al concentrations in the same filter digests as for the REF-Fe analysis using the VG Elemental PlasmaQuad-2 (PQ2+) ICP-MS at ULB, equipped with a Cetac Aridus desolvating sample introduction system, which was upgraded with a PFA microconcentric nebulizer (100 μL/min) and PFA spray chamber. External calibration was done with standards in 0.05 M $HNO_3$ and Sc as internal standard. Filter digestion blanks amounted to 17.4 ± 4.0 ng Al (1 SD, n = 3) resulting in a detection limit (3 SD of filter blank) of 12 ng. To validate the digestion method for Al, we analyzed DC-75301 and found 6.78 ± 0.42% (2 SD, n = 3, certified value DC-75301 6.92 ± 0.22%, recovery 98%).

The filter blanks for REF-Fe and REF-Al contributed between <1% and 30% to the measured concentrations.

In the following we will present the Fe data as the measured parameters TD-Fe, DFe and REF-Fe, as well as the derived parameters total Fe (TOT-Fe = TD-Fe + REF-Fe) and particulate labile Fe (PL-Fe = TD-Fe − DFe). It should be noted that PL-Fe is a highly operationally defined parameter, which depends on the strength and type of acid, the length of time and temperature of storage, and the type of particles in the unfiltered sample (Berger et al., 2008). It serves here to illustrate trends in labile and refractory Fe. DFe represents a size cut-off of 0.2 μm and may also contain, apart from free ionic Fe, (in)organic colloidal Fe, nanoparticulate Fe as well as truly soluble (in)organic Fe complexes. REF-Al data serve as an indicator of lithogenic input, with REF-Fe/REF-Al ratios as a useful tool to identify sources and sinks of the refractory particulate phase.

### 3.3. Additional parameters

Bulk sea ice salinity, temperature and Chl *a* were determined by standard techniques described in Rémy et al. (2008). Water depths at the sea ice stations were estimated from a bathymetric map provided by Land Information New Zealand (LINZ).

## 4. Results

### 4.1. Sea ice physics

Two types of sea ice could be discerned: first-year land-fast ice at Stations 1, 2 and 5, and multi-year land-fast ice at Stations 3, 4 and 6 (Fig. 2). The ice texture of the first-year ice is characteristic for land-fast ice near an ice shelf (Gow et al., 1998), with granular ice near the surface, followed by columnar ice and finally platelet ice. Station 1 near Cape Evans did not exhibit platelet ice, probably because of a submarine ridge between Cape Evans and Inaccessible Island (Dellbridge Islands) inhibiting supercooled ISW to enter this zone (Smith et al., 2001). Multi-year ice is thicker and the sequence of columnar ice and platelet ice is repeated. Also, layers containing a mix of columnar and platelet ice are observed at Stations 5 and 6 (Fig. 2).

The temperature profiles ranged between −1.5 °C and −3.8 °C (Fig. 3A, B). Bulk salinities varied between 0 and 12 (Fig. 3C, D). The relative brine volumes, calculated cf. Cox and Weeks (1983), ranged between 0 and 30% (Fig. 3E, F). First-year sea ice and multi-year sea ice exhibit different physical characteristics in terms of thickness, temperature, bulk salinity and porosity (Rémy et al., 2008) and shapes of the profiles of these parameters. As expected the first-year sea ice is thinner than multi-year sea ice (i.e., 198 ± 11 cm (n = 3) versus 326 ± 30 cm (n = 3)) and warmer, with a difference of about 1 °C (Fig. 3A, B). The minimum temperatures are found just below the top layer, all stations showing signs of warming at the very surface, which may be an effect of sampling at the warmest part of the day. The temperature in the

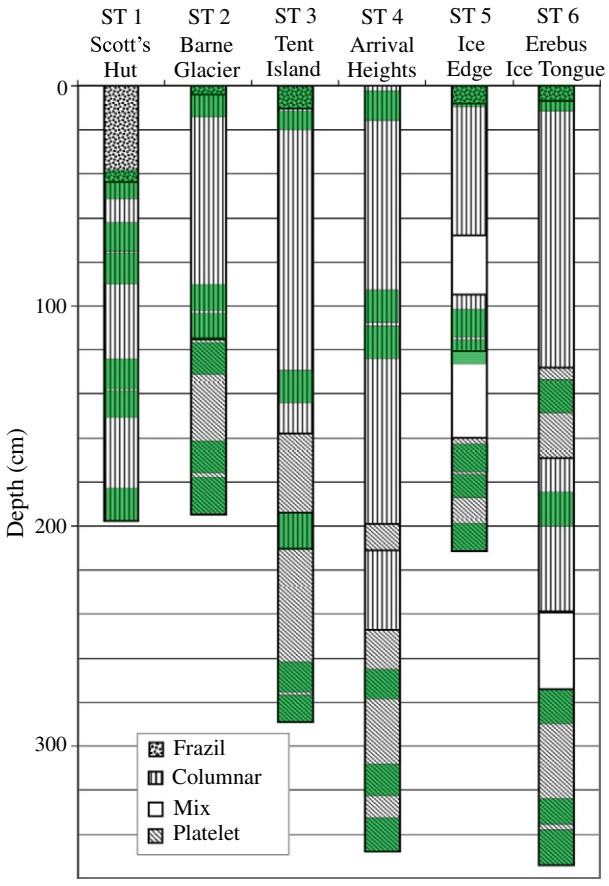


**Fig. 2.** Ice textures for each occupied station (Rémy, 2005). In green are indicated the depths at which sample slices were processed for Fe analyses.

bottom ice (defined as the ice at the bottom of the sea ice cover) is approaching that of the seawater freezing temperature.

Multi-year sea ice appears to be less porous and less saline, particularly in the upper part of the cores (Fig. 3D, F). This is due to desalination of the sea ice by brine drainage, causing a departure from the typical C-shaped profiles of first-year sea ice (Fig. 3C). Relative brine volumes in the first-year sea ice cores amounted to 12.0 ± 3.9%. Relative brine volumes higher than 5% are indicative of the development of a well-connected brine channel network (Golden et al., 1998). The thicker multi-year ice had lower relative brine volumes (7.6 ± 4.9%), with stations 3 and 6 having brine volumes well below the 5% threshold in the upper meter of the cores, meaning that the brine channel system can be considered impermeable and less prone to exchange processes. The bottom ice at all stations is very porous with brine volumes of 20–30% (Fig. 3E, F).

It should be noted that multi-year sea ice is not typical for this part of McMurdo Sound, and that its occurrence is likely to have been caused by a subtle interplay between storm events and location of the blockading iceberg B-15 (Brunt et al., 2006).

### 4.2. Biology

In the upper parts of the cores dinoflagellates (notably *Polarella glacialis*) were predominantly found, while in the bottom ice pennate diatoms (*Amphiprora* sp. and *Nitzschia stellata*) dominated the microbial community (Rémy et al., 2008). Maximum Chl *a* abundance was observed in the bottom ice (Table 3) with the highest value of 42 μg/L at Station 1. First-year sea ice exhibited on average higher maximum Chl *a* concentrations (29 ± 12 μg/L) than the multi-year sea ice (17 ± 11 μg/L), likely due to light limitation caused by the thicker ice (Rémy et al., 2008). The multi-year sea ice exhibited maximum values near the bottom ice but Chl *a* strongly decreased in the last centimeters of ice (Table 3). We surmise that this was due to new growth of platelet ice, which may have been responsible for isolating the original bottom ice community to be replaced with a secondary community whose growth was light-limited due to self-shading.

### 4.3. Iron distributions

#### 4.3.1. Snow

Snow was thin or absent due to strong wind ablation. At the stations where snow samples could be collected (Stations 1, 2, 4 and 6), high Fe concentrations were found (Table 4). By far the highest concentrations were found at Station 4 in the close vicinity of McMurdo Station, the next highest concentrations were found at near-shore station 1. Concentration ranges were 112–2410 nmol/L DFe, 198–7282 nmol/L PL-Fe, 45–3624 nmol/L REF-Fe, and 151–5829 nmol/L REF-Al. Microscopic examination of the particulate matter on the polycarbonate membrane filters after filtration of the melted snow revealed a mix of quartz sand and gray and red gravel (not shown). Molar Fe/Al ratios in the refractory particulate material decreased linearly with distance from McMurdo station (Fig. 4), from 0.61 at Station 4 to 0.29 at Station 2, 30 km away to the north–northwest.

#### 4.3.2. Land-fast ice

The Fe profiles in the sea ice generally had a C-shape (Fig. 5, Table 4), with the highest concentrations at the top and at the bottom of the ice core. Intermediate depths were generally the lowest in concentration. First-year sea ice (Stations 1, 2 and 5) exhibited 2.2–109 nmol/L DFe, 7.6–586 nmol/L PL-Fe, 1.3–116 nmol/L REF-Fe and 8.6–470 nmol/L REF-Al, while for multi-year sea ice (Stations 3, 4 and 6) this was 2.9–72 nmol/L DFe, 6.6–1106 nmol/L PL-Fe, 2.0–749 nmol/L REF-Fe and 10–1462 nmol/L REF-Al.

The average depth integrated inventories (Table 5) for whole cores follow generally similar tendencies with equal inventories for DFe, a twice larger inventory for PL-Fe and a four times larger inventory for REF-Fe in multi-year ice, compared to first-year ice.

Median refractory Fe/Al ratios and their median absolute deviations (MAD: median of absolute deviations from the data's median (Hampel, 1974)) were 0.29 ± 0.09 (n = 17) for sea ice with Chl *a* <0.5 μg/L and 0.51 ± 0.11 (n = 11) for sea ice with Chl *a* >0.5 μg/L (Table 1). Median and MAD were used as they provide typical values and robust estimates of data dispersion (i.e., relatively insensitive to outliers).

#### 4.3.3. Under-ice seawater

The under-ice Fe concentrations at the different stations ranged between 0.3–3.6 nmol/L DFe, 0.5–15 nmol/L PL-Fe and <DL–5.4 nmol/L REF-Fe (Table 4). Irrespective of station position we observed a linear increase of all concentrations with time (Fig. 6). We estimated increases of DFe by 0.52 nmol/L/d ($R^2$ = 0.78, p = 0.044), of PL-Fe by 2.4 nmol/L/d ($R^2$ = 0.96, p = 0.003) and of REF-Fe by 0.89 nmol/L/d ($R^2$ = 0.85, p = 0.027). REF-Al did not show a significant correlation with time ($R^2$ = 0.19, p = 0.55). However, a linear trend was observed for the refractory Fe/Al ratio, which increased from around 0.14 until 0.30 within a week's time (Fig. 6), resulting in a rate of 0.042 per day ($R^2$ = 0.97, p = 0.11).

## 5. Discussion

### 5.1. Iron concentrations in snow, sea ice and under-ice seawater

Antarctic pack ice and land-fast ice exhibit Fe concentrations one to two orders of magnitude higher than the underlying seawater (Table 6). Iron inputs to Antarctic sea ice are generally low (Lannuzel et al., 2007,

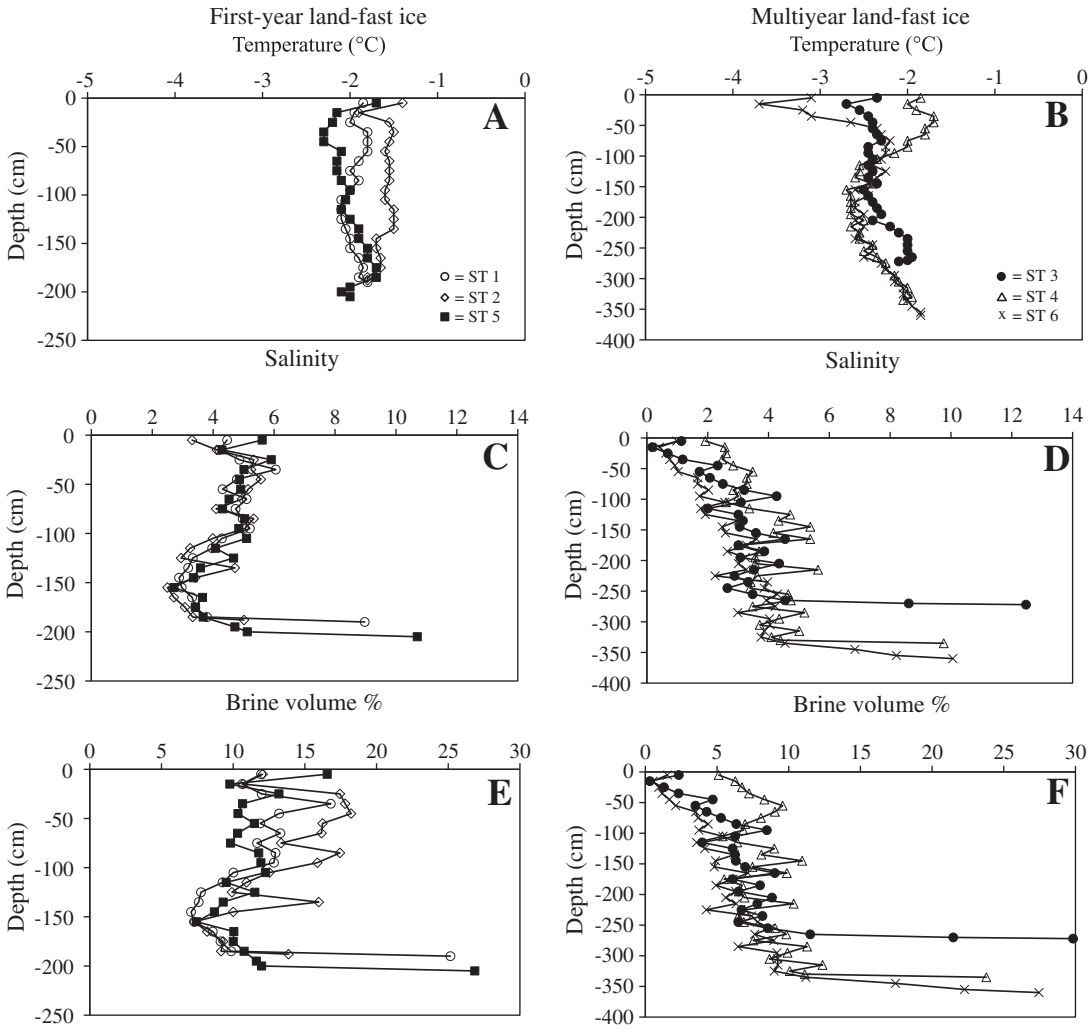


**Fig. 3.** Temperature (A, B), salinity (C, D), and brine volume (E, F) profiles along the ice cores of first-year ice (left) and multi-year ice (right) (Rémy, 2005).

2008, 2010) due to the fact that Antarctica is very isolated from other landmasses, has no river runoff, has very little exposed rock and soil as well as a relatively deep continental shelf. Atmospheric dust inputs are generally very small (except McMurdo Sound), and the pathways of loading sea ice with Fe are thus mainly limited to lateral diffusion/advection from benthic fluxes in coastal areas and vertical diffusion/advection of Fe rich deep waters (de Jong et al., 2012).

The snow Fe concentrations that we have found in McMurdo Sound, are exceptionally high when compared with other Antarctic studies (Table 6). This is due to a combination of local sources of atmospheric dust, notably the snow-free McMurdo Dry Valleys, wind-blown material from the MIS, soil perturbation at McMurdo Station and Erebus volcano. The only other study reporting very high Fe concentrations in Antarctica is by Ikegawa et al. (1997). They observed concentrations in the range of this study at Asuka station near the Sør Rondane Mountains during austral spring 1991, which were attributed to two simultaneous huge volcanic eruptions, notably Mt. Pinatubo and Cerro Hudson, although a more local crustal source like the Sør Rondane Mountains should not be excluded (see Section 5.3 for a further treatment of atmospheric inputs).

Iron distributions in land-fast ice and seawater that we report here for the McMurdo Sound, can be compared with studies by Grotti et al. (2005) in nearby Terra Nova Bay (Ross Sea) and by van der Merwe et al. (2011a, 2011b) in East-Antarctic waters (Table 6). van der Merwe et al. (2011a) sampled one land-fast ice site at a water depth of 380 m and 75 km offshore, and found Fe concentrations in all fractions that were on the whole lower than observed in our study as well as in studies by van der Merwe et al. (2011b) and Grotti et al. (2005). The sampling sites of our study and the studies by van der Merwe et al. (2011b) and Grotti et al. (2005) can be directly compared, as they consist both of land-fast ice, are within 2 km of the coast and have similar shallow water depths of less than 500 m.

The under-ice seawater DFe concentrations of all studies exhibit similar ranges of concentrations (0.1–4.5 nmol/L). However, comparing the particulate Fe concentrations in seawater with those in land-fast sea ice and open ocean pack ice suggests a link with the proximity of the coast (Table 6), indicating that the particulate Fe distribution in land-fast ice is influenced by lithogenic sources, such as the sediment and/or wind-blown dust.

Comparison of median concentrations between first-year and multi-year sea ice (Table 7) allows us to look in more detail at the Fe distribution as a function of sea ice type (i.e., granular, columnar, non-bottom platelet and bottom (platelet or columnar)). From top to bottom of the ice cores, the following can be observed (Table 7).

Iron concentrations in granular ice are relatively high in all fractions, compared to the columnar ice further down-core. No significant difference was observed between first-year and multi-year ice. Granular sea ice Fe shows high variability, this may be due to the possible percolation of high Fe snowmelt into the granular ice at the top of the ice which for instance may have been the case at Station 6. Columnar ice and (non-

**Table 3**
Chlorophyll *a* concentrations.

| | Depth (cm) | Chl *a* (μg/L) |
|---|---|---|
| *First-year sea ice* | | |
| ST1: Scott's hut | 11 | 0.05 |
| | 82 | 0.11 |
| | 95 | 0.36 |
| | 134 | 0.26 |
| | 143 | 0.29 |
| | 194 | 41.74 |
| ST2: Barne Glacier | 11 | 0.02 |
| | 102 | 0.02 |
| | 110 | 0.03 |
| | 118 | 0.03 |
| | 180 | 7.33 |
| | 187 | 26.71 |
| ST5: Ice Edge | 4 | 0.17 |
| | 113 | 0.50 |
| | 116 | 0.29 |
| | 206 | 17.92 |
| *Multi-year sea ice* | | |
| ST3: Tent Island | 4 | 0.20 |
| | 12 | 0.08 |
| | 158 | 1.06 |
| | 278 | 28.54 |
| | 286 | 2.61 |
| ST4: Arrival Heights | 11 | 0.10 |
| | 107 | 0.40 |
| | 114 | 2.12 |
| | 322 | 5.30 |
| | 345 | 0.10 |
| ST6: Erebus Ice Tongue | 3 | 0.10 |
| | 143 | 0.25 |
| | 291 | 1.86 |
| | 337 | 21.86 |
| | 344 | 10.41 |
| | 351 | 2.79 |

bottom) platelet ice exhibit the lowest Fe concentrations of all ice types. Columnar ice DFe and PL-Fe are significantly lower in multi-year ice as compared with first-year ice (t-test, 95% confidence level), probably for reasons of brine drainage that drives desalination in multi-year ice. REF-Fe was not significantly different between multi-year ice and first-year ice, suggesting that refractory material may have been more incorporated into the sea ice lattice and therefore less sensitive to brine drainage. PL-Fe is likely associated with biofilm gel (Becquevort et al., 2009) in brine pockets and brine channels, as well as the walls thereof, while DFe is to be found in the brine liquid (van der Merwe et al., 2011a). This makes both fractions sensitive to changes in relative brine volume, but due to greater mobility of DFe a decoupling in the release of PL-Fe and DFe may occur during sea ice melt (van der Merwe et al., 2011a). Contrastingly, non-bottom platelet ice in multi-year ice is significantly higher (t-test, 95% confidence level) in DFe, PL-Fe and REF-Fe values than in first-year ice. All the non-bottom platelet ice layers in the multi-year ice belong to the second-year new growth phase (the exception is station 6/135–149 cm, not further taken into account here. This layer consists probably of remnant bottom platelet ice from the first year ice growth. Its concentrations resemble those of columnar ice also due to brine drainage). As the multi-year sea ice stations are located in generally shallower waters, the observed difference may be due to stronger scavenging by buoyant platelet ice of suspended particulate matter derived from sediment resuspension in these higher turbidity waters.

The highest Fe concentrations in all fractions are generally associated with the bottom ice, whether columnar bottom ice (station 1) or platelet bottom ice (all other stations). Bottom ice PL-Fe in multi-year ice is 12× higher than in first-year ice, while bottom ice REF-Fe is 6× higher than in first-year ice (Table 7). PL-Fe is higher not only because sea ice algae in multi-year bottom ice had more time to scavenge DFe from a generally shallower water column, but they probably also scavenged DFe that came down from the upper layers of the ice during brine drainage. A part of this biologically scavenged Fe may subsequently be transformed in more refractory Fe phases (see Section 5.4).

With respect to the relative contribution of PL-Fe to total particulate Fe, given as PL-Fe/(PL-Fe + REF-Fe), we find that first-year ice (83 ± 7%, n = 18) and multi-year ice (67 ± 12%, n = 17) are significantly different (t-test, 95% confidence level). This suggests not only that more PL-Fe has been transformed into refractory Fe species in multi-year ice, but also that more suspended sedimentary material has been incorporated into the ice due to the shallower waters in which the multi-year ice was present. Overall, these PL-Fe percentages are high for marine suspended particulate matter. We find similar values for seawater (68 ± 16%, n = 5) and for snow (74 ± 7%, n = 4). If we compare these with data from the open Ross Sea by Coale et al. (2005), who used an acetic acid leaching technique of filtered suspended particulate material, PL-Fe represents only 8 ± 7% (n = 188). One reason for this difference may be the operationally defined nature of determining PL-Fe. Berger et al. (2008) presented evidence that the acetic acid leaching technique of collected particles is too weak, but that the dissolvable method, which was applied here, may be too harsh, i.e. it would also attack a part of the residual fraction and would thus overestimate the potentially bioavailable exchangeable Fe fraction. It could also be argued that the PL-Fe percentages presented here are realistic and that they are high in the sea ice due to the strong cycling of Fe by the biota present in the sea ice, and high in wind-blown dust in the snow because of the low degree of Fe oxidation of the bedrock source material. This is due to very slow chemical weathering (Mahaney et al., 2009) in the region, leading to relatively high proportions of Fe bearing minerals to be in the ferrous form. Once into contact with aqueous media (snow melt, seawater) this reduced Fe rapidly dissolves, but also rapidly oxidizes to secondary Fe oxyhydroxide phases that may be easily exchangeable. Suspended particulate matter of McMurdo Sound would probably have high PL-Fe due to the biogenic nature of the surface sediment (Dunbar et al., 1989).

### 5.2. Under-ice sources of Fe

The observation of the under-ice seawater Fe concentrations increasing linearly during the sampling period (Fig. 6) could be explained by several mechanisms. A first possibility is sea ice melting. This would mean that despite the physical differences between the stations and the variable Fe concentrations at the different stations, the drainage of Fe from the melting sea ice would steadily increase independent of site and/or becoming rapidly mixed within the upper mixed layer of the whole of Erebus Bay. At the rates by which Fe concentrations were increasing in the seawater, and given the sea ice Fe inventories, the sea ice would be completely depleted of all Fe within 5 days, if sea ice drainage was the only source of Fe to the water column. Iron depletion is not what we observe in the sea ice and we therefore have to consider additional sources.

A second possibility is that a sediment resuspension event was taking place, affecting the eastern slopes of Southern McMurdo Sound. Sediment resuspension is a well-known phenomenon in McMurdo Sound (Leventer and Dunbar, 1987), resulting in a pervasive near-bottom nepheloid layer of 25 to 250 m thick (Dunbar et al., 1989) and usually more common in winter (Dunbar et al., 1989; Berkman et al., 1986). In order to explain the observed increases of 0.52 nmol/L/d DFe, 2.4 nmol/L/d PL-Fe and 0.89 nmol/L/d REF-Fe in an ~400 m water column, fluxes across the sediment–water interface are required of 208 μmol/m$^2$/d DFe, 960 μmol/m$^2$/d PL-Fe and 356 μmol/m$^2$/d REF-Fe. For DFe, similar sediment flux ranges have been reported in literature, for instance for the Pacific continental margin by Elrod et al. (2004) (range 1.3–10.8 μmol/m$^2$/d) and Severmann et al. (2010) (range 6–568 μmol/m$^2$/d), while Blain et al. (2008) report a value for the subantarctic Kerguelen island shelf of 136 μmol/m$^2$/d. Other values for

**Table 4**
Fe and Al concentrations in land-fast ice of McMurdo Sound.

| | Layer cm | Ice type | DFe nmol/L | TD-Fe nmol/L | PL-Fe nmol/L | REF-Fe nmol/L | TOT-Fe nmol/L | REF-Al nmol/L | REF Fe/Al |
|---|---|---|---|---|---|---|---|---|---|
| ST1 | Snow | | 295 | 2192 | 1897 | 675 | 2866 | 1888 | 0.36 |
| 16-01-2003 | 38–52 | G/C | 23 | 147 | 125 | 28 | 176 | 153 | 0.19 |
| First-year | 62–76 | C | 20 | 82 | 63 | 12 | 94 | 55 | 0.21 |
| | 76–90 | C | 10 | 55 | 44 | 6 | 61 | 32 | 0.20 |
| | 125–139 | C | 24 | 130 | 107 | 17 | 147 | 44 | 0.38 |
| | 139–153 | C | 20 | 68 | 48 | 5 | 73 | 20 | 0.27 |
| | 181–195 | C | 107 | 168 | 61 | 32 | 201 | 57 | 0.58 |
| | Seawater | | 0.26 | 0.80 | 0.54 | <DL | 1.5 | 9 | – |
| ST2 | Snow | | 155 | 354 | 198 | 45 | 399 | 153 | 0.30 |
| 17-01-2003 | 2–17 | G/C | 34 | 119 | 85 | 11 | 130 | 23 | 0.48 |
| First-year | 92–102 | C | 9.3 | 63 | 53 | 17 | 79 | 59 | 0.30 |
| | 102–116 | C | 7.0 | 29 | 22 | 4.3 | 33 | 15 | 0.30 |
| | 117–131 | P | 2.2 | 13 | 11 | 3.6 | 16 | 27 | 0.14 |
| | 161–175 | P | 2.8 | 10 | 7.6 | 1.5 | 12 | 10 | 0.15 |
| | 175–189 | P | 29 | 108 | 79 | 25 | 133 | 63 | 0.43 |
| | seawater | | 0.91 | 2.2 | 1.3 | <DL | 2.4 | <DL | – |
| ST3 | Snow | | – | – | – | – | – | – | – |
| 18-01-2003 | 0–10 | G | 16 | 79 | 63 | 27 | 106 | 96 | 0.29 |
| Multi-year | 11–20 | C | 3.7 | 12 | 8.4 | 5.3 | 17 | 11 | 0.54 |
| | 150–163 | C | 5.6 | 17.1 | 11 | 4.4 | 21 | <DL | – |
| | 194–210 | C | 9.2 | 27.1 | 18 | 8.1 | 35 | 56 | 0.16 |
| | 262–275 | P | 58 | 131 | 73 | 28 | 159 | 52 | 0.59 |
| | 276–291 | P | 72 | 1178 | 1106 | 749 | 1927 | 1602 | 0.51 |
| | Seawater | | 1.2 | 7.9 | 6.7 | 3.0 | 11 | 25 | 0.14 |
| ST4 | Snow | | 2410 | 9692 | 7282 | 3624 | 13316 | 5948 | 0.62 |
| 14-01-2003 | 2.5–16.5 | C | 2.9 | 20 | 17 | 7.8 | 28 | 33 | 0.25 |
| Multi-year | 93–107 | C | 4.1 | 33 | 29 | 20 | 53 | 23 | 0.95 |
| | 109–123 | C | 10 | 137 | 126 | 68 | 205 | 127 | 0.58 |
| | 265–279 | P | 20 | 106 | 86 | 32 | 138 | 121 | 0.29 |
| | 308–322 | P | 13 | 148 | 135 | 49 | 197 | 222 | 0.25 |
| | 329–341 | P | 62 | 1058 | 996 | 197 | 1255 | 386 | 0.58 |
| | Seawater | | – | – | – | – | – | – | – |
| ST5 | Snow | | – | – | – | – | – | – | – |
| 22-01-2003 | 0–11 | G | 83 | 542 | 459 | 116 | 658 | 481 | 0.25 |
| First-year | 102–114 | C | 22 | 81 | 59 | 12 | 93 | 20 | 0.63 |
| | 114–125 | C/P | 14 | 96 | 82 | 10 | 107 | 17 | 0.70 |
| | 164–175 | P | 11 | 80 | 69 | 9.6 | 89 | 16 | 0.69 |
| | 175–186 | P | 27 | 80 | 53 | 7.7 | 88 | 18 | 0.50 |
| | 199–211 | P | 109 | 695 | 586 | 53 | 748 | 90 | 0.67 |
| | Seawater | | 3.7 | 18 | 15 | 5.2 | 23 | 22 | 0.30 |
| ST6 | Snow | | 112 | 742 | 630 | 206 | 948 | 568 | 0.40 |
| 19-01-2003 | 0–13 | G/C | 52 | 477 | 425 | – | – | – | – |
| Multi-year | 135–149 | P | 8.2 | 23 | 15 | 1.8 | 25 | 14 | 0.20 |
| | 186–200 | C | 4.8 | 11 | 6.6 | 4.3 | 16 | 32 | 0.20 |
| | 275–289 | P | 20 | 61 | 41 | 26 | 87 | 97 | 0.40 |
| | 324–335 | P | 24 | 288 | 264 | 89 | 377 | 377 | 0.37 |
| | 335–346 | P | 62 | 150 | 88 | 174 | 323 | 844 | 0.34 |
| | Seawater | | 0.54 | 8.1 | 7.6 | 4.0 | 12 | 51 | 0.15 |

G: granular ice.
P: platelet ice.
C: columnar ice.

coastal marine sediments are not much different, e.g., Pakhomova et al. (2007) measured fluxes in the Gulf of Finland between 5 and 1000 μmol/m$^2$/d while Epping et al. (1998) measured between 20 and 1440 μmol/m$^2$/d in an intertidal area of the coastal North Sea. Sediments have thus a clear potential to explain the inferred fluxes. These fluxes are also more than sufficiently large to fuel the observed Fe inventory of the sea ice. The increase in Fe/Al ratios in the under-ice seawater supports the sea ice–sediment link for Fe supply. These ratios increased from 0.14, a low value in the range of those for biogenic opal (Table 8) suggesting the presence of diatom frustules, to 0.30, which is close to local marine sediment values (Table 1). This suggests a shift from biogenic suspended particulate material in the water column to more lithogenic suspended particulate material. Moreover, there is a good linear correlation between water depth at the stations and the internal sea ice inventories of REF-Fe and REF-Al, with highest inventories in the shallowest waters (Fig. 7). The exception of Station 1 as the only station without platelet ice underscores the importance of platelet ice scavenging of lithogenic material. The absence of correlations of DFe and PL-Fe inventories in sea ice versus water depth (not shown) could indicate that these fractions in sea ice undergo internal transformations resulting in a balance struck between production and loss terms. Dissolved Fe production results from dissolution of particulate Fe by photoreduction, organic complexation, viral lysis, bacterial remineralization, zooplankton grazing, and protozoa ingestion (Hassler and Schoemann, 2009). Loss of DFe occurs through brine drainage and biological uptake/particle scavenging (i.e., conversion to PL-Fe or REF-Fe) (Lannuzel et al., 2007, 2008). An indication of DFe loss through brine drainage can be found in the observation that the salinity and relative brine volumes are about a factor two to three lower in the upper half of the cores of multi-year ice, as compared with first-year ice (Fig. 3). This desalination leads to similar DFe concentrations and inventories in both first-year ice and multi-year ice.

A sediment resuspension event could have been triggered by tidal forcing in McMurdo Sound. Tides in McMurdo Sound have a diurnal

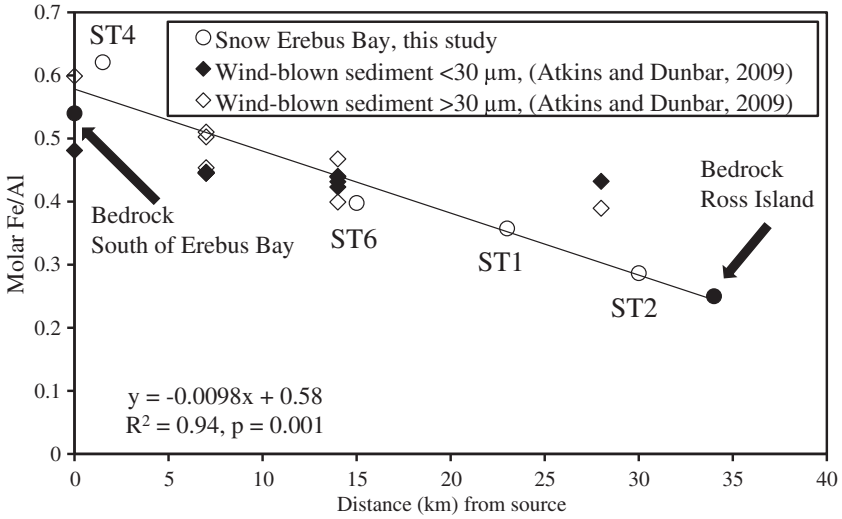


**Fig. 4.** Decreases of molar Fe/Al with distance from the MIS in wind-blown dust on sea ice of central McMurdo Sound (Atkins and Dunbar, 2009), and with distance from McMurdo Station in refractory particulate matter of snow in Erebus Bay (this study). Linear regression line is for snow data and Erebus Bay lithogenic end members (soil McMurdo station and rock outcrops Cape Royds) and concerns the open and closed circles only.

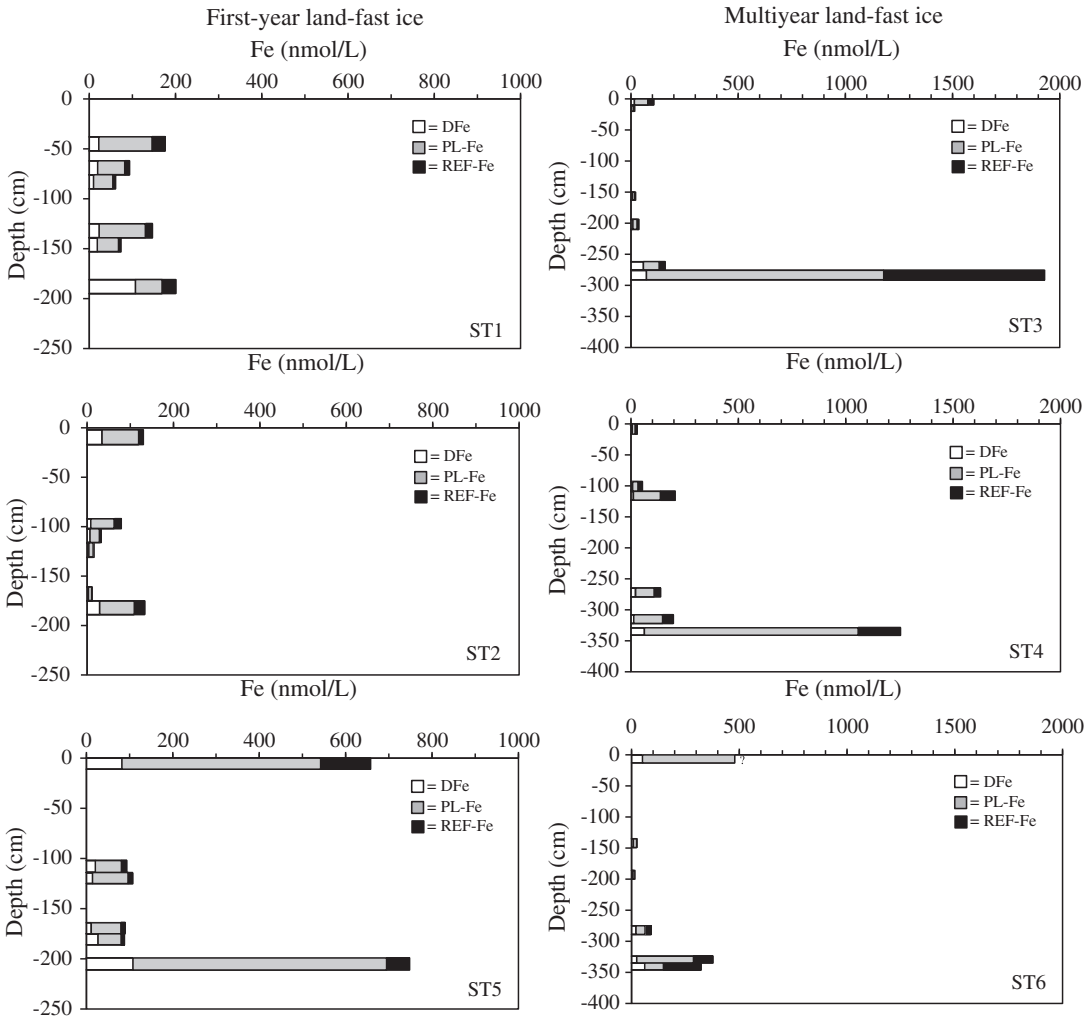


**Fig. 5.** Dissolved, particulate leachable and refractory Fe profiles along the ice cores of first-year ice land-fast (left) and multi-year land-fast ice (right). Note the different concentration scales between first-year and multi-year ice.

**Table 5**
Depth integrated Fe and Al inventories of McMurdo sea ice.

| Station # | DFe μmol/m² | | PL-Fe μmol/m² | | REF-Fe μmol/m² | | TOT-Fe μmol/m² | | TOT-Fe μmol/m² | % DFe of TOT-Fe | % of TOT-Fe | REF-Al μmol/m² | |
|---|---|---|---|---|---|---|---|---|---|---|---|---|---|
| | SI | S | SI | S | SI | S | SI | S | SI + S | SI + S | S | SI | S |
| *First-year* | | | | | | | | | | | | | |
| 1 | 63 | 29 | 161 | 190 | 36 | 67 | 260 | 287 | 546 | 17% | 52% | 141 | 188 |
| 2 | 30 | 16 | 91 | 20 | 19 | 5 | 140 | 40 | 180 | 25% | 22% | 59 | 16 |
| 5 | 64 | – | 275 | – | 42 | – | 382 | – | – | – | – | 97 | – |
| *Multi-year* | | | | | | | | | | | | | |
| 3 | 49 | – | 234 | – | 143 | – | 426 | – | – | – | – | 307 | – |
| 4 | 47 | 241 | 427 | 728 | 154 | 362 | 627 | 1332 | 1959 | 15% | 68% | 356 | 583 |
| 6 | 77 | 11 | 446 | 63 | 69 | 21 | 591 | 95 | 686 | 13% | 14% | 204 | 51 |
| *First-year* | | | | | | | | | | | | | |
| Average | 52 | | 176 | | 32 | | 260 | | | | | 99 | |
| SD | 20 | | 93 | | 12 | | 121 | | | | | 41 | |
| *Multi-year* | | | | | | | | | | | | | |
| Average | 58 | | 369 | | 122 | | 548 | | | | | 289 | |
| SD | 17 | | 117 | | 46 | | 107 | | | | | 78 | |

SI: sea ice.
S: snow.

cycle with a period between spring and neap tide of 13.66 days (Goring and Pyne, 2003). The sampling period of this study coincided with a spring tide phase (Robinson et al., 2010), which may have induced resuspension of the sediments due to strong bottom currents (Leventer and Dunbar, 1987; Berkman et al., 1986).

Rising platelet ice may assist in upward transport of biogenic and terrigenous debris (Dunbar et al., 1989). A sub-surface layer of platelet ice may have been present during our sampling period in summer 2003, provoked by the unique condition of iceberg B-15 blocking McMurdo Sound since 2000. At the time of sampling, waters underneath the MIS were below the surface freezing temperature of seawater along the whole water column (Robinson et al., 2010). Robinson et al. (2010) also observed a tongue with the coldest waters at decreasing depths (350 m to 250 m), in function of upward sloping of the underside of the ice shelf, which may have extended into McMurdo Sound as a source of platelet ice formation. Suspended platelet ice was collected under the eastern MIS (Robinson et al., 2010), as well as under a sea ice station in front of the MIS, not far from our Station 4 (Robinson, 2004). Moreover, the multi-year sea ice stations show indications of new platelet ice growth as Chl *a* (Table 3) and other biological parameters (Rémy et al., 2008) decrease at the ice–seawater interface.

### 5.3. Atmospheric input

McMurdo Sound is subject to various sources of atmospheric input, leading to high Fe concentrations in snow (Table 4). The Fe inventories in snow (Table 5) are 11–241 μmol/m² DFe, 20–728 μmol/m² PL-Fe and 5–362 μmol/m² REF-Fe. The total snow Fe inventory of 40–1332 μmol/m² TOT-Fe represents between 14% and 68% of the total sea ice Fe inventory with the lowest contributions at the stations the furthest offshore from Ross Island (18 ± 6%, Stations 2 and 5) and the highest for the stations closest to shore (60 ± 11%, Stations 1 and 4). We will further discuss flux estimates in the following sub-sections.

#### 5.3.1. McMurdo Dry Valleys

Dust and gravel are blown into the coastal zone by westerly foehn winds from the McMurdo Dry Valleys. Lancaster (2002) reported average values of total wind-blown dust fluxes in the Dry Valleys to vary

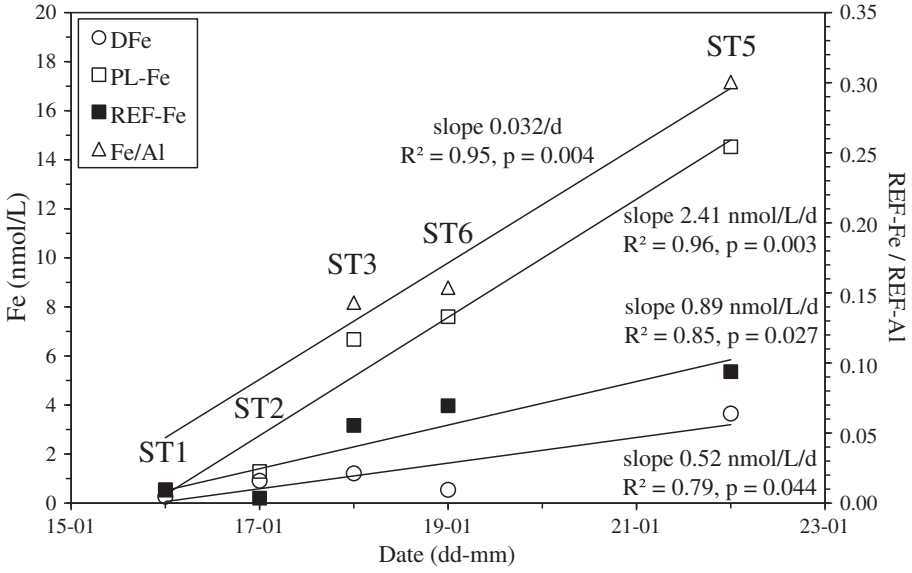


**Fig. 6.** Increases with time in under-ice seawater of DFe, PL-Fe, REF-Fe and molar Fe/Al in the refractory particulate matter.

**Table 6**
Overview of reported Fe concentrations (nmol/L) in snow, pack ice, land-fast ice and under-ice seawater.

| Sample type | DFe | TD-Fe | PFe | Region | Reference |
|---|---|---|---|---|---|
| Snow | 112–2410 | 354–9692 | 243–10906 [a] | Ross Sea, McMurdo Sound | This study |
| | – | – | 11–7831 | East-Antarctica, Asuka Station | Ikegawa et al. (1997) |
| | – | – | 20.1 | East-Antarctica, Dome C | Boutron and Martin (1980) |
| | 0.2–1.1 | 0.7–6.9 | 1.1–12 | East-Antarctica | van der Merwe et al. (2011a) |
| | 0.9–7.1 | 9.6–47 | 2.3–101 | East-Antarctica | van der Merwe et al. (2011b) |
| | 1.0–6.5 | 1.8–24 | 2.1–15 | East-Antarctica | Lannuzel et al. (2007) |
| | – | 0.8–21 | – | East-Antarctica | Edwards and Sedwick (2001) |
| | 0.7–3.2 | 7.8–22 | 7.8–14 | Weddell Sea | Lannuzel et al. (2008) |
| | – | 31–53 | – | Weddell Sea | Löscher et al. (1997) |
| | – | 4.5–16 | – | Weddell Sea | Westerlund and Öhman (1991) |
| | 0.3–1.0 | 1.0–5.9 | – | Bellingshausen Sea | Lannuzel et al. (2010) |
| Pack ice | 0.2–14 | 1.2–104 | 0.9–78 | East-Antarctica | van der Merwe et al. (2011a) |
| | 2.6–26 | 3.3–112 | <DL–97 | East-Antarctica | Lannuzel et al. (2007) |
| | 0.7–37 | 2.3–98 | 2.3–141 | Weddell Sea | Lannuzel et al. (2008) |
| | 2.8–25 | 95 | – | Weddell Sea | Boyé et al. (2001), de Baar and de Jong (2001) |
| | – | 11–99 | – | Weddell Sea | Löscher et al. (1997) |
| | 0.4–30 | 1.7–78 | – | Bellingshausen Sea | Lannuzel et al. (2010) |
| Land-fast ice | 2.2–109 | 10–1178 | 9.0–1854 [a] | Ross Sea, McMurdo Sound | This study |
| | 1.1–6.0 | – | 26–1162 | Ross Sea, Terra Nova Bay | Grotti et al. (2005) |
| | 0.8–2.1 | 17–378 | 7.5–215 | East-Antarctica | van der Merwe et al. (2011a) |
| | 2.1–81 | 34–4240 | 40–6830 | East-Antarctica | van der Merwe et al. (2011b) |
| Seawater | 0.3–3.7 | 0.8–18 | 1.1–20[a] | Ross Sea, McMurdo Sound | This study |
| | 0.7–1.5 | – | 28–45 | Ross Sea, Terra Nova Bay | Grotti et al. (2005) |
| | 0.4–4.2 | – | 1.1–59 | Ross Sea, Terra Nova Bay | Grotti et al. (2001) |
| | 0.1–2.6 | 0.4–7.4 | 0.1–2.9 | East-Antarctica | van der Merwe et al. (2011a) |
| | 1.5–3.7 | 12–48 | 11–60 | East-Antarctica | van der Merwe et al. (2011b) |
| | 1.1–4.5 | 1.3–3.8 | <DL–4.4 | East-Antarctica | Lannuzel et al. (2007) |
| | 0.7–1.7 | 0.5–4.1 | 0.4–4.0 | Weddell Sea | Lannuzel et al. (2008) |
| | 0.1–0.6 | 0.3–1.6 | – | Bellingshausen Sea | Lannuzel et al. (2010) |

[a] For comparability derived from PL-Fe + REF-Fe.

from a sand-dominated maximum of 442 g/m$^2$/yr at valley floors to a minimum of silt/clay-dominated 0.26 g/m$^2$/yr on glaciers at higher elevations, with a median value of 3.7 g/m$^2$/yr. Wind-blown dust deposition to the coastal zone of the Dry Valleys has been estimated to be as high as 6.5 g/m$^2$/yr (Ayling and McGowan, 2006).

### 5.3.2. McMurdo Ice Shelf

The MIS is characterized by the presence of dirty ice bands consisting of boulders, clay, sand and gravel, which have been incorporated into the basal ice by adfreezing and transported upward by ablation (Atkins and Dunbar, 2009). The Southern McMurdo Sound facing the MIS experiences fall-out from this wind-blown material, which is visible as an elongate dirty lobe on the sea ice downwind of the MIS (Atkins and Dunbar, 2009). A remarkably high load of wind-blown material of 24.5 g/m$^2$/yr directly in front of the MIS was estimated, decreasing to 7.8 g/m$^2$/yr at a 20 km distance (Atkins and Dunbar, 2009). Smaller aerosol sources to McMurdo Sound consist of exposed surface sediments at Black Island, White Island and Minna Bluff, located 30–70 km south of Ross Island. Accumulation of wind-blown material from these sources in Windless Bight directly south of Ross Island was estimated at 0.80 g/m$^2$/yr (Dunbar et al., 2009).

**Table 7**
Typical Fe concentrations per sea ice type.[a]

| Sea ice type | DFe nmol/L | PL-Fe nmol/L | REF-Fe nmol/L | REF-Al nmol/L | n |
|---|---|---|---|---|---|
| *First-year ice* | | | | | |
| Granular | 34 ± 12 | 125 ± 39 | 28 ± 18 | 152 ± 129 | 3 |
| Columnar | 17 ± 6 | 56 ± 10 | 11 ± 5 | 25 ± 11 | 8 |
| Non-bottom platelet | 7 ± 4 | 32 ± 23 | 6 ± 3 | 15 ± 4 | 4 |
| Bottom (platelet or columnar) | 107 ± 1 | 79 ± 18 | 32 ± 7 | 58 ± 3 | 3 |
| *Multi-year ice* | | | | | |
| Granular | 34 ± 18 | 244 ± 181 | 27 | 94 | 2 (1) |
| Columnar | 5 ± 1 | 17 ± 9 | 8 ± 3 | 27 ± 17 | 7 |
| Non-bottom platelet | 20 ± 4 | 86 ± 45 | 32 ± 6 | 109 ± 61 | 5 |
| Bottom (platelet) | 62 ± 1 | 996 ± 109 | 196 ± 23 | 510 ± 173 | 3 |

[a] Median ± MAD. MAD is the median absolute deviation, meaning the median of the absolute deviations from the data's median.

### 5.3.3. Mount Erebus volcano

Volcanic activity consisted during the last decades of degassing of an active lava lake in the summit's crater and frequent low-intensity Strombolian eruptions (up to 6 per day) (Kelly et al., 2008) from the lava lake or subsidiary vents, from which a persistent volcanic plume

**Table 8**
Refractory and bulk Fe/Al ratios in biogenic marine material.

| Sample type | Location | Depth | Median | MAD | n | Reference |
|---|---|---|---|---|---|---|
| Refractory SPM[a] | Ross Sea, spring | <100 m | 0.41 | 0.06 | 22 | Coale et al. (2005) |
| | | >100 m | 0.30 | 0.05 | 29 | |
| Refractory SPM | Ross Sea, summer | <100 m | 0.56 | 0.18 | 28 | |
| | | >100 m | 0.35 | 0.07 | 34 | |
| Refractory SPM | ACC[b], spring | <100 m | 0.41 | 0.04 | 10 | |
| | | >100 m | 0.52 | 0.08 | 25 | |
| Refractory SPM | ACC, summer | <100 m | 0.64 | 0.19 | 24 | |
| | | >100 m | 0.55 | 0.18 | 22 | |
| Refractory SPM | South of Crozet Islands | 30–340 m | 1.07 | 0.11 | 5 | Planquette et al. (2009) |
| Refractory SPM | Near Crozet Islands | | 0.52 | 0.01 | 3 | |
| Refractory SPM | North of Crozet Islands | | 0.66 | 0.13 | 13 | |
| Sample type | Location | Material | Median | MAD | n | Reference |
| Sediment | ACC | Biogenic opal | 0.08 | 0.04 | 32 | Ellwood and Hunter (2000) |
| Sediment core-top | ACC, NW Pacific Ocean | Biogenic opal | 0.07 | 0.02 | 6 | Shemesh et al. (1988) |
| Plankton net tows | NE Pacific Ocean | Diatom frustules | 0.13 | 0.05 | 14 | Martin and Knauer (1973) |

[a] SPM: suspended particulate matter.
[b] ACC: Antarctic Circumpolar Current.

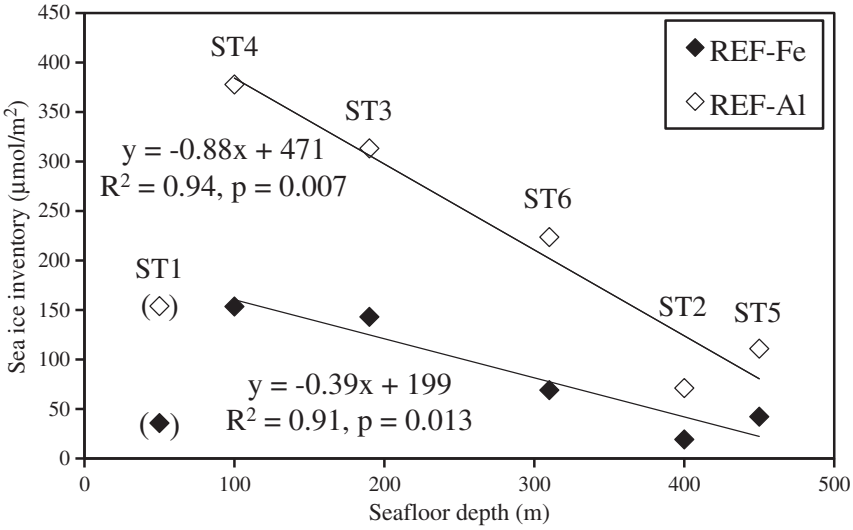


**Fig. 7.** Sea ice inventories of REF-Fe and REF-Al, as a function of seafloor depth. Between brackets is Station 1, the only station without platelet ice (see text).

emanates, which disperses widely across the Ross Sea and Ross Ice Shelf (Kyle et al., 1990; Chuan et al., 1986). Airborne measurements conducted by Chuan et al. (1986) in December 1983 led to a particle flux estimation of 21.3 ± 3 metric ton/d. Alternatively, using $SO_2$ fluxes as obtained by Kyle et al. (1990) in December 1984 as well as reported Al/S ratios in particles collected on the crater rim, and the Al abundance (10.6%) of the magma, we calculated a particle flux of 7.7 ± 4.7 metric ton/d. It is probable that the bulk of the volcanic ash is transported out to the open Ross Sea as a result of the predominantly southerly winds, without so much as affecting the direct surroundings of the volcano, also given the fact that the ash is injected into the atmosphere at a 3800 m altitude (Chuan et al., 1986). Assuming that 50% of the ejected volcanic particles are larger than 20 µm and will fall out within a semi-circular area with a radius of 300 km as in Chuan et al. (1986), small deposition rates of only 0.010–0.028 g/m$^2$/yr could be deduced. Only atmospheric fall-out from large eruptions would have a noticeable effect on the marine biogeochemistry of the region.

*5.3.4. Ross Island*

The total Fe concentrations in the snow particulate matter together with refractory Fe/Al ratios (assuming that these are the same for total Fe/Al ratios) and the total Al abundance in the source material from McMurdo soil (7.5 ± 0.1%, value used for Stations 4 and 6) (Crockett, 1998) and from western Ross Island volcanic rock (9.5 ± 1.3%, value used for Stations 1 and 2) (Kyle, 1976), allowed us to approximate the accumulation rate of wind-blown material in Erebus Bay. Assumptions were made for snow deposition rate (0.69 kg/m$^2$/d) (Braaten, 1997) and snow density (500 kg/m$^3$) (Braaten, 1997), as well as snow wind erosion and snow sublimation (5% and 9%, respectively) (van Lipzig et al., 2004). The wind-blown dust fluxes amounted in descending order to 3.4 g/m$^2$/yr (Station 4), 1.0 g/m$^2$/yr (Station 1), 0.30 g/m$^2$/yr (Station 6) and 0.17 g/m$^2$/yr (Station 2).

It is likely that the particulate matter accumulated on the snow at Station 4 was derived from soil perturbation by human activity at McMurdo Station (Crockett, 1998), blown there by the predominantly easterly winds at this site (Mazzera et al., 2001). When considering a PM10 aerosol concentration (atmospheric particulate matter < 10 µm) of 4 µg/m$^3$ at McMurdo Station (Mazzera et al., 2001) and a deposition velocity of 2 cm/s for mineral dust in a coastal environment (Duce et al., 1991), a dust deposition rate of 2.5 g/m$^2$/yr can be deduced. Despite large uncertainties in the deposition velocity, this is in reasonable agreement with our findings for nearby Station 4, giving confidence in the result we obtained. The high value at Station 4 corresponds less well with the 0.80 g/m$^2$/yr reported by Dunbar et al. (2009) for nearby Windless Bight on the other side of Hut Point Peninsula, which is understandable as this area lies upwind from Hut Point Peninsula and receives dust from sources further away (such as Minna Bluff, Black Island and White Island).

The provenance of particles accumulated in the snow at Station 1 is likely exposed soil and rock from the western shore of Ross Island and its adjacent small islands (Fig. 1B). This is supported by a trend in the refractory Fe/Al ratios versus distance from McMurdo Station (Fig. 4). It shows a linearly decreasing trend, which can be interpreted as a mixing line between a basanitic signature from the south of Erebus Bay (median Fe/Al = 0.54, Table 1) to lower Fe/Al further north derived from wind-blown material of more phonolitic compositions of Ross Island (median Fe/Al = 0.25) (Table 1). A similar mixing line as discussed above can also be seen in the Fe/Al descending trend of the wind-blown dust on the sea ice in central Southern McMurdo Sound (data in supplementary material in Atkins and Dunbar (2009)), which is located to the west of Erebus Bay. Fe/Al in particles >30 µm descends within the first 15 km northward of the dirty ice of the MIS from 0.6 to 0.4 along a similar slope as our data. Fe/Al in particles <30 µm remains constant at a ratio of about 0.44. As of 15 km away and beyond, Fe/Al <30 µm and >30 µm converge and remain constant at levels of Fe/Al = 0.41. This leveling-off suggests a particle size sorting effect on Fe/Al with increasing distance from the source and may indicate the increased presence of fine wind-blown dust with Fe/Al = 0.41, typical of sources in the Dry Valleys west of McMurdo Sound (Table 1), brought in by westerly foehn winds. Summarizing, these results suggest a dust mixing in Erebus Bay between sources to the south and to the east, contrasting with dust mixing in Southern McMurdo Sound involving sources to the south and to the west. Dust from the Dry Valleys thus seems not to be deposited in significant amounts at our sampling sites in Erebus Bay, but would probably be deposited further to the west.

In conclusion, the estimated atmospheric fluxes for Erebus Bay are high compared with those found elsewhere in Antarctica (in the range of only 0.004–0.2 g/m$^2$/yr) (e.g., Wagener et al., 2008; McConnell et al., 2007; Planquette et al., 2007). The atmospheric dust sources in our study area appear to be predominantly local and can be associated with areas where rock and soil lie exposed to the wind and/or human soil perturbation occurs on the western shores of Ross Island. The magnitude of these dust sources (0.17–3.4 g/m$^2$/yr) is significantly higher compared to an estimated 0.010–0.028 g/m$^2$/yr from Erebus volcano, but lower compared to wind-blown dust fluxes into the western McMurdo Sound from the Dry Valleys (3.7–6.5 g/m$^2$/yr) (Ayling and McGowan, 2006; Lancaster, 2002) and the MIS (7.8–24.5 g/m$^2$/yr) (Atkins and Dunbar, 2009). These dust fluxes, while taking into account

the specific Fe abundances of the different source areas, translate into TOT-Fe deposition rates of 30–93 μmol/m$^2$/d (MIS, 7.8% Fe), 11–19 μmol/m$^2$/d (western McMurdo Sound, 5.9% Fe), 0.48–9.5 μmol/m$^2$/d (Erebus Bay, 5.7% Fe) and 0.019–0.053 μmol/m$^2$/d (Erebus volcano, 3.9% Fe). Assuming a dissolution rate of 5% in seawater, atmospheric DFe fluxes to open waters in McMurdo Sound would amount to 1.5–4.7 μmol/m$^2$/d (MIS), 0.54–0.94 μmol/m$^2$/d (western and central McMurdo Sound), 0.024–0.48 μmol/m$^2$/d (Erebus Bay) and 0.0010–0.0027 μmol/m$^2$/d (Erebus volcano). These fluxes can be compared with the benthic Fe fluxes as derived from our water column data, which during spring tide can be as high as ~200 μmol/m$^2$/d DFe or ~1500 μmol/m$^2$/d TOT-Fe. This comparison suggests that the sediment could be by far the most important Fe source to the sea ice in McMurdo Sound. However, this is not taking into account the efficiency by which this Fe supply will be associated with the sea ice cover. The TOT-Fe inventory in snow in Erebus Bay varies between 40 and 1332 μmol/m$^2$ (Table 5). Assuming a 9 month ice cover, this inventory would require a flux of 0.15–4.9 μmol/m$^2$/d to be built up. The actual atmospheric Fe fluxes are in the range of 0.48–9.5 μmol/m$^2$/d, implying that 30–50% of the atmospheric Fe supply to the snow remains on the ice, while the rest is further dispersed with the prevailing winds towards the Ross Sea by wind ablation of snow and saltation of particles. In the case of sediment incorporation into the sea ice, the TOT-Fe inventory in sea ice in Erebus Bay is on average 260 ± 121 μmol/m$^2$ for first-year ice (Table 5). If we take an initial rapid sea ice growth phase of 1 week at growth rates exceeding 10 cm per day (Leonard et al., 2006) during which most of the particulate matter becomes trapped in the ice (Garrison et al., 1986), a flux of about 40 μmol/m$^2$/d TOT-Fe would be required to build up the sea ice inventory. The actual benthic TOT-Fe flux was as large as 1500 μmol/m$^2$/d, suggesting that 2.5% of the benthic Fe supply to the sea ice from below should become retained in the ice. This estimate does not take into account an unknown amount of Fe, which is lost due to spring melt, so the actual winter inventory is probably higher and scavenging efficiency as well. Also, this estimate is calculated with a benthic Fe flux which was at its highest during a spring tide sediment resuspension event. In between these tidal events, the benthic Fe flux is probably much lower and therefore the scavenging efficiency may be higher. This estimate may however represent an upper limit, because the land-fast ice cover continues to thicken at reduced growth rates of less than 1 cm per day for the duration of several months longer (Leonard et al., 2006; Purdie et al., 2006). This further growth is likely to allow for further scavenging of resuspended benthic particulate matter during phases of platelet ice formation in mid-winter, but to what extent remains unknown. Also unknown is the amount of DFe sequestered by the biota dwelling in the sea ice, and transferred to PL-Fe and/or REF-Fe phases, which contributes as well to the built-up of the Fe inventory of the sea ice.

Comparison of the Fe concentrations in snow and in the top layers of the land-fast ice, shows that the high snow signal does not become incorporated into the sea ice or at least not very deeply, as snow-ice formation conditions (such as seawater flooding due to a thick snow cover followed by refreezing) were absent in the McMurdo area. Enhanced Fe concentrations were found in the top layers of the sea ice only at Stations 5 and 6 (Fig. 5). Higher temperatures were registered on the sampling dates of Stations 5 and 6 (Table 2), which could have induced some snowmelt and percolation of the Fe enriched melt water into the surface layers of the sea ice. Unfortunately, we neither have snow Fe/Al at Station 5 nor top layer Fe/Al at Station 6 to establish a direct atmospheric link between high Fe concentrations in snow and the top layer of the ice cores at Stations 5 and 6.

### 5.4. Particulate Fe/Al ratios in bottom ice

The variation of refractory Fe/Al with depth in sea ice cores shows distinct signatures between layers with high and layers with low Chl *a* present (Tables 1, 3 and 4). Median values of 0.29 ± 0.09 (n = 17) for sea ice with Chl *a* <0.5 μg/L may reflect the signature of sediment-derived material as sediments in McMurdo Sound and the western Ross Sea exhibit a median value of around 0.32 (Table 1). Significantly higher median values of 0.51 ± 0.11 (n = 11) for sea ice with Chl *a* >0.5 μg/L (t-test, 95% confidence level) were typically found in bottom ice, but also in some intermediate layers with remnant Chl *a* at multi-year sea ice Stations 3 and 4, and cannot be explained with the sediment Fe/Al signature. These high Fe/Al ratios could be caused by two processes. A first possibility is linkage with the abundance of sea ice algae (pennate diatoms) in the bottom ice. The REF-Fe enrichment relative to REF-Al may be due to biological Fe uptake and/or passive Fe adsorption by the diatoms. Biological uptake involves incorporation of Fe in metal activated proteins and enzymes as well as refractory metalloproteins and storage products, which may resist chemical attack (Collier and Edmond, 1984). Adsorption of Fe is likely to occur on diatom cell surfaces (Sunda, 2001; Collier and Edmond, 1984) in the form of poorly crystalline hydrous ferric oxide (HFO). The adsorbed HFO may upon aging convert into more crystalline and refractory Fe oxyhydroxides such as hematite, α-FeOOH and γ-FeOOH (Sunda, 2001).

An alternative explanation for the higher observed refractory Fe/Al in bottom ice is a linkage to a source to the south of lithogenic material with a suitably high Fe/Al ratio, such as could be derived from melting of the base of the MIS cavity, and transported to our research area further north in supercooled ISW. This lithogenic material may be scavenged into the bottom ice during platelet ice formation. Contradicting this explanation is however the observation that high Fe/Al is not limited to bottom platelet ice only, but also occurs in columnar bottom ice (Station 1) and intermediate columnar ice layers with remnant Chl *a* (Stations 3 and 4). As described above, we observed a significant correlation between sea ice inventories of REF-Fe or REF-Al and water depth suggesting that the local sediments are the dominating source rather than a more remote source from under the MIS. Enhanced terrigenous suspended particulate matter associated with mid-water cold tongues of melt water from a small glacier terminus has indeed been observed to penetrate only about 1 km into the adjacent ocean (Domack et al., 1994), making it unlikely that sedimentary particles from basal melting could be transported several tens of kilometers away from the ice shelf terminus without sedimenting out again. An alternative source of lithogenic material from basal melting of ice shelves or glaciers could be the nearby Erebus Ice Tongue (Dunbar et al., 1989) in Erebus Bay. However, the lithogenic material from the east side of McMurdo Sound has a low Fe/Al ratio of 0.25 (Table 1), which makes it an unlikely candidate.

High refractory Fe/Al ratios in biogenic suspended particulate matter have been observed before. Refractory Fe and Al data from Coale et al. (2005) for suspended particulate matter from the Ross Sea and the Antarctic Circumpolar Current revealed for both contrasting marine settings (i.e., continental shelf sea versus open ocean) an increase of the refractory Fe/Al ratio in the upper 100 m from spring to summer (Table 8), while deep water (>100 m) Fe/Al remained constant. This is consistent with the notion of biological uptake during the ongoing summer blooms and transfer into a refractory biogenic Fe pool. Refractory Fe and Al data reported by Planquette et al. (2009) indicated terrigenous refractory Fe/Al ratios of 0.52 in suspended particulate matter close to the Crozet Islands in the Southern Ocean, typical of their bedrock composition of about 0.51, and more biogenic values upstream (1.07) and downstream (0.66) of the islands (Table 8). However, not all kinds of biogenic particulate matter will show high refractory Fe/Al ratios, as is the case for diatomaceous opal. Published Fe/Al ratios in opal from carefully washed sediments and plankton net tows (Table 8) indicate a Fe/Al ratio of biogenic opal of 0.13 and lower. The refractory particulate matter in bottom ice in McMurdo Sound likely contains a mix of biogenic and sediment-derived lithogenic material. The biogenic refractory material probably consists of diatomaceous opal and a 'soft-tissue' related refractory fraction (organics such as metalloproteins and storage products, as well as authigenic oxyhydroxides either as precipitates or as coatings).

### 5.5. Biogeochemical importance of McMurdo Sound sea ice for primary productivity in the Ross Sea

The sea ice from McMurdo Sound, Fe-rich from sedimentary inputs and loaded with wind-blown dust in its snow, may provide an important source of Fe to the Ross Sea when the usual sea ice breakout occurs in Spring. With the combined sea ice + snow cover inventory of TOT-Fe in McMurdo Sound at the various stations ranging between 180 and 1959 μmol/m$^2$ (Table 5), and taking an area of 55 × 55 km for sea ice covered McMurdo Sound at the end of winter, the sea ice contains 30–331 metric tons of Fe. If we consider the fraction of DFe in snow and sea ice (average 17 ± 5%; Table 5) as representative for its solubility, then McMurdo Sound land-fast ice has a potential of bringing 5.2–56 metric tons of soluble Fe into the Ross Sea when it breaks out and melts in spring. Indeed, observations have confirmed enrichment with dissolved and particulate Fe to various degrees of the upper mixed layer of the Ross Sea in sea ice covered waters (e.g., Rivaro et al., 2011, 2012; Grotti et al., 2001; Sedwick et al., 2000). Iron release from melting sea ice takes place gradually, but this happens over a relatively short time period without necessarily complete meltdown of the sea ice (Lannuzel et al., 2008). Taken over a period of 30 days (Lannuzel et al., 2008), the release of the snow + sea ice DFe inventory of 45–288 μmol/m$^2$ (Table 5) would lead to fluxes of 1.5–9.6 μmol/m$^2$/d DFe. This is higher than previous estimates for open ocean pack ice by Lannuzel et al. (2007, 2008) for East-Antarctic waters (0.30 μmol/m$^2$/d) and the Weddell Sea (0.38 μmol/m$^2$/d). However, the dispersion of the sea ice from McMurdo Sound into the larger Ross Sea would diminish the flux. Based on the surface circulation in the western Ross Sea (see Sedwick et al., 2011), we may assume that the land-fast ice from McMurdo Sound spreads out in spring to the north along the western shore of the Ross Sea. The McMurdo Sound DFe inventory would thus give rise to a flux of approximately 0.050–0.32 μmol/m$^2$/d DFe if we assume that the spreading area covers 20% of the entire surface of the Ross Sea (450,000 km$^2$). This comes on top of a melting flux of the already present open ocean pack ice, which is likely to exhibit DFe fluxes of around 0.3 μmol/m$^2$/d (Lannuzel et al., 2007, 2008). Thus melting land-fast ice from McMurdo Sound could potentially double the DFe flux of melting sea ice to the western Ross Sea. This underlines the importance of sedimentary and atmospheric inputs to land-fast ice from McMurdo Sound as a vector for natural Fe fertilization to the Ross Sea.

In the following paragraph we compare the DFe flux from land-fast and pack ice melt with other DFe sources to the Ross Sea. Sedwick et al. (2011) measured in spring and summer depleted concentrations of DFe in the western Ross Sea. They suggested significant sources of new DFe to reconcile low DFe with the observation of significant biomass accumulation in the Ross Sea Polynya, namely 1) particulate Fe, which is rendered bioavailable through dissolution, photoreduction and biological processing; 2) vertical exchange with iron-rich deep waters; 3) horizontal advection and lateral redistribution of DFe derived from sea ice melt and shallow benthic sources; and 4) aerosol deposition and dissolution. The role of particulate Fe as a source of DFe for primary productivity remains largely unknown. Photochemically-mediated dissolution is not well constrained. Regenerative dissolution of particulate Fe by ingestion of biogenic or lithogenic particles by protozoa (Barbeau et al., 1996) and zooplankton (such as copepods and krill) (Tovar-Sanchez et al., 2007; Sarthou et al., 2008; Schmidt et al., 2011) has been shown to play an important role in the oceanic Fe cycle (e.g., Boyd et al., 2005). Also recycling at higher trophic levels (sea birds, sea mammals) (Nicol et al., 2010) has been proposed. The following recycling flux estimates of DFe have been reported: 0.006–0.076 μmol/m$^2$/d (krill, Schmidt et al., 2011) and 0.039 μmol/m$^2$/d (whales, de Jong et al., 2012, using Nicol et al., 2010). Regarding vertical exchange, Coale et al. (2005) have estimated vertical upwelling of 0.027 μmol/m$^2$/d. Horizontal advective/diffusive DFe flux from shallow benthic sources may range between 0.010 and 0.10 μmol/m$^2$/d DFe on a scale of 1000 km, if we take a recent estimate for the Antarctic Peninsula into account (de Jong et al., 2012). As seen above, the dispersion of McMurdo Sound land-fast ice to the Ross Sea could attribute 0.050–0.32 μmol/m$^2$/d to an already present flux of 0.30–0.38 μmol/m$^2$/d from melting open ocean pack ice. In the close vicinity of individual melting McMurdo Sound ice floes, this flux could be considerably higher. As for aerosol DFe deposition to the Ross Sea, if the dust load in the snow on the sea ice in McMurdo Sound represents only 50% of what has been blown across McMurdo Sound (see Section 5.3), then the fraction blown away across the Ross Sea would bring a flux of 0.0002–0.006 μmol/m$^2$/d DFe. Volcanic activity from Mount Erebus would attribute 0.001–0.003 μmol/m$^2$/d (Erebus volcano). Aerosol DFe deposition to the southern central Ross Sea was estimated by Edwards and Sedwick (2001) at 0.0016 μmol/m$^2$/d, which is in the range of what we report here. Icebergs were not taken into consideration here as a source of DFe, as the melting rate would be vanishingly small in the subzero waters of the Ross Sea.

A DFe budget for the western Ross Sea (Table 9) shows that melting sea ice (land-fast and pack ice) could contribute 84–90% of the supply of new DFe. The DFe released into the surface ocean by sea ice melting is likely to be bioavailable due to the high concentrations of saccharides in sea ice (Dumont et al., 2009). Saccharides form highly bioavailable organic associations with iron, which increase Fe solubility, mainly as colloidal Fe (Hassler et al., 2011), and render Fe more bioavailable than other naturally occurring organic ligands (Hassler et al., 2011; Hassler and Schoemann, 2009).

The sum of new DFe sources was used to estimate the regenerative DFe flux from the microbial loop (Table 9) using an average *fe* ratio of 0.33, based on values of 0.17 by Boyd et al. (2005) and 0.49 by Sarthou et al. (2008). To this was added krill grazing (Schmidt et al., 2011) and higher trophic level recycling by whales (Nicol et al., 2010). The total DFe flux consisting of new DFe and recycled DFe fluxes, which is thus estimated at 1.2–2.7 μmol/m$^2$/d (Table 9), could be used to calculate the potentially sustainable primary productivity. The outcome depends on the choice of Fe/C ratio to convert Fe supply into primary productivity. Applying a range of between 10 μmol/mol and 40 μmol/mol (cf. Hassler and Schoemann, 2009; de Baar et al., 2008; Sarthou et al., 2005) would yield primary production rates of 1.5–3.2 and 0.37–0.79 gC/m$^2$/d, respectively. These results are in good agreement with values of primary productivity reported by Arrigo and van Dijken (2003) for the Ross Sea Polynya, which are in the range of 0.5–2 gC/m$^2$/d.

The fact that the seasonal breakout of land-fast ice out of McMurdo Sound and into the western Ross Sea happened much less or not at all

**Table 9**
Fe budget for the Ross Sea.

| | DFe flux μmol/m$^2$/d | % contribution new DFe | Reference |
|---|---|---|---|
| *New DFe flux* | | | |
| Vertical upwelling/diffusion | 0.027 | 3–7% | Coale et al. (2005) |
| Horizontal advection/diffusion | 0.010–0.10 | 3–12% | de Jong et al. (2012) |
| Melting land-fast ice McMurdo | 0.050–0.32 | 13–38% | This study |
| Melting open ocean pack ice | 0.30–0.38 | 77–45% | Lannuzel et al. (2007, 2008) |
| Sum of melting sea ice | 0.35–0.70 | 90–84% | |
| Blown snow McMurdo Sound | 0.0002–0.006 | 0.1–0.7% | This study |
| Mount Erebus volcano | 0.001–0.003 | 0.3–0.4% | This study |
| Total | 0.39–0.84 | | |
| *Regenerative DFe flux* | | | |
| Microbial loop, avg. *fe* = 0.33 | 0.79–1.7 | | Boyd et al. (2005), Sarthou et al. (2008) |
| Krill grazing | 0.006–0.076 | | Schmidt et al. (2011) |
| Higher trophic level recycling | 0.039 | | Nicol et al. (2010) |
| Total | 0.83–1.8 | | |
| Grand total | 1.2–2.7 | | |

during the blockade of the giant icebergs B-15 and C-19 may have led to greater Fe limitation in the Ross Sea. Also, horizontal advection/diffusion from continental shelf sources of DFe may have been perturbed by the presence of these icebergs. The heavy pack ice conditions due to the icebergs led to the late opening of the Ross Sea Polynya, with severe light limitation of the phytoplankton and a shorter blooming period as a consequence. Iron/light co-limitation may have been the cause of observed negative effects on abundance and structure of the phytoplankton community (Arrigo and van Dijken, 2003; Arrigo et al., 2002) leading to strongly suppressed primary productivity rates to one third of the normal levels. Heavy pack ice conditions and reduced primary productivity also impacted the structure and abundance of the higher trophic levels (e.g., pteropods, krill, fish, penguins) (Arrigo and van Dijken, 2003).

## 6. Conclusion

In this paper we presented new data on Fe in snow, land-fast ice and under-ice seawater of Erebus Bay in the eastern part of McMurdo Sound. Dissolved and particulate concentrations in the sea ice were two to three orders of magnitude higher than in the underlying seawater. A general increase in seawater dissolved and particulate Fe could be ascribed to sediment resuspension due to tidal forcing during bimonthly periods of spring tides. We propose that entrainment of sediment derived Fe is the most important pathway for high Fe concentrations in land-fast ice. Iron fluxes from the sediment were estimated and could fully account for the Fe inventory of the sea ice. Wind-blown dust in the snow on the sea ice makes up for 14–68% of the total Fe inventory of the sea ice, but does not appear to contribute to the Fe content of the sea ice proper. The largest sources of wind-blown dust to the sea ice in western and central McMurdo Sound are the MIS and the Dry Valleys, but in the eastern McMurdo Sound (Erebus Bay) exposed rock and soil at Ross Island are the major sources of atmospheric inputs. The usual spring breakup of sea ice to the Ross Sea may have a significant potential fertilizing effect on the waters of the Ross Sea. This was demonstrated by budget calculations and deduced from the strong diminution of primary production in the Ross Sea in the absence of this breakup due to the blocking presence of the giant icebergs B-15 and C-19.

## Acknowledgments

We are indebted to Antarctica New Zealand for hosting us and to the crew at Scott Base for logistical support. This study would not have been possible without the financial support from the ARC-SIBCLIM project (contract no. ARC-2/07-287) funded by the Belgian French Community, and the BELCANTO project (contract no. SD/CA/03A) funded by the Belgian Federal Science Policy Office. We are also grateful to the Fonds de la Recherche Scientifique (F.R.S.-FNRS, Belgium) for support of the MC-ICP-MS facility at ULB under the FRFC contract no. 2.4617.06. The detailed comments by four anonymous reviewers helped to improve this manuscript.

## References

Ackley, S.F., Sullivan, C.W., 1994. Physical controls on the development and characteristics of Antarctic sea ice biological communities — a review and synthesis. Deep-Sea Res. I 41, 1583–1604.
Arrigo, K.R., van Dijken, G.L., 2003. Impact of iceberg C-19 on Ross Sea primary production. Geophys. Res. Lett. 30. http://dx.doi.org/10.1029/2003GL017721.
Arrigo, K.R., van Dijken, G.L., Ainley, D.G., Fahnestock, M.A., Markus, T., 2002. Ecological impact of a large Antarctic iceberg. Geophys. Res. Lett. 29. http://dx.doi.org/10.1029/2001GL014160.
Atkins, C.B., Dunbar, G.B., 2009. Aeolian sediment flux from sea ice into southern McMurdo Sound, Antarctica. Glob. Planet. Chang. 69, 133–141.
Ayling, B.F., McGowan, H.A., 2006. Niveo-eolian sediment deposits in coastal South Victoria Land, Antarctica: indicators of regional variability in weather and climate. Arct. Antarct. Alp. Res. 38, 313–324.
Barbeau, K., Moffett, J.W., Caron, D.A., Croot, P.L., Erdner, D.L., 1996. Role of protozoan grazing in relieving iron limitation of phytoplankton. Nature 380, 61–64.
Barry, J.P., Dayton, P.K., 1988. Current patterns in McMurdo Sound, Antarctica, and their relationship to local biotic communities. Polar Biol. 8, 367–376.
Becquevort, S., Dumont, I., Tison, J.L., Lannuzel, D., Sauvée, M.L., Chou, L., Schoemann, V., 2009. Biogeochemistry and microbial community composition in sea ice and underlying seawater off East Antarctica during early spring. Polar Biol. 32, 879–895.
Berger, C.J.M., Lippiatt, S.M., Lawrence, M.G., Bruland, K.W., 2008. Application of a chemical leach technique for estimating labile particulate aluminum, iron, and manganese in the Columbia River plume and coastal waters off Oregon and Washington. J. Geophys. Res. 113, C00B01. http://dx.doi.org/10.1029/2007JC004703.
Berkman, P.A., Marks, D.S., Shreve, G.P., 1986. Winter sediment resuspension in McMurdo Sound, Antarctica, and its ecological implications. Polar Biol. 6, 1–3.
Bertler, N.A.N., Mayewski, P.A., Barrett, P.J., Sneed, S.B., Handley, M.J., Kreutz, K.J., 2004. Monsoonal circulation of the McMurdo Dry Valleys, Ross Sea region, Antarctica: signal from snow chemistry. Ann. Glaciol. 39, 139–145.
Bishop, J.L., Lougear, A., Newton, J., Doran, P.T., Froeschl, H., Trautwein, A.X., Körner, W., Koeberl, C., 2001. Mineralogical and geochemical analyses of Antarctic lake sediments: a study of reflectance and Mössbauer spectroscopy and C, N, and S isotopes with applications for remote sensing on Mars. Geochim. Cosmochim. Acta 65, 2875–2897.
Blain, S., Sarthou, G., Laan, P., 2008. Distribution of dissolved iron during the natural iron-fertilization experiment KEOPS (Kerguelen Plateau, Southern Ocean). Deep-Sea Res II 55, 594–605.
Bockheim, J.G., 2002. Landform and soil development in the McMurdo Dry Valleys, Antarctica: a regional synthesis. Arct. Antarct. Alp. Res. 34, 308–317.
Boutron, C., Martin, S., 1980. Sources of twelve trace metals in Antarctic snows determined by principal component analysis. J. Geophys. Res. 85 (C10), 5631–5638.
Boyd, P.W., Law, C.S., Hutchins, D.A., Abraham, E.R., Croot, P.L., Ellwood, M., et al., 2005. FeCycle: attempting an iron biogeochemical budget from a mesoscale SF6 tracer experiment in unperturbed low iron waters. Global Biogeochem. Cycles 19, GB4S20. http://dx.doi.org/10.1029/2005GB002494.
Boyd, P.W., Jickells, T., Law, C.S., Blain, S., Boyle, E.A., Buesseler, K.O., et al., 2007. Mesoscale iron enrichment experiments 1993–2005: synthesis and future directions. Science 315, 612–617.
Boyé, M., van den Berg, C.M.G., de Jong, J.T.M., Leach, H., Croot, P., de Baar, H.J.W., 2001. Organic complexation of iron in the Southern Ocean. Deep-Sea Res. I 48, 1477–1497.
Braaten, D.A., 1997. A detailed assessment of snow accumulation in katabatic wind areas on the Ross Ice Shelf, Antarctica. J. Geophys. Res. 102 (D25), 30047–30058.
Brunt, K.M., Sergienko, O., MacAyeal, D.R., 2006. Observations of unusual fast-ice conditions in the southwest Ross Sea, Antarctica: preliminary analysis of iceberg and storminess effects. Ann. Glaciol. 44, 183–187.
Bull, J.R., 2009. Stable Isotope, Major and Trace Element Chemistry of Modern Snow from Evans Piedmont Glacier, Antarctica: Insights into Potential Source Regions and Relationship of Glaciochemistry to Atmospheric Circulation and Vigour. Master thesis Victoria University of Wellington, New Zealand 207.
Chuan, R.L., Palais, J., Rose, W.I., Kyle, P.R., 1986. Fluxes, sizes, morphology and compositions of particles in the Mt. Erebus volcanic plume, December 1983. J. Atmos. Chem. 4, 467–477.
Coale, K.H., Gordon, R.M., Wang, X., 2005. The distribution and behavior of dissolved and particulate iron and zinc in the Ross Sea and Antarctic Circumpolar Current along 170°W. Deep-Sea Res. I 52, 295–318.
Collier, R., Edmond, J., 1984. The trace element geochemistry of marine biogenic particulate matter. Prog. Oceanogr. 13, 113–199.
Comiso, J.C., 2003. Variability and trends of the global sea ice cover. In: Thomas, D.N., Dieckmann, G.S. (Eds.), Sea Ice, an Introduction to its Physics, Chemistry, Biology and Geology. Chichester, Wiley-Blackwell, pp. 205–246.
Cooper, A.F., Adam, L.J., Coulter, R.F., Eby, G.N., McIntosh, W.C., 2007. Geology, geochronology and geochemistry of a basanitic volcano, White Island, Ross Sea, Antarctica. J. Volcanol. Geoth. Res. 165, 189–216.
Cox, G.F.N., Weeks, W.F., 1983. Equations for determining the gas and brine volumes in sea ice samples. J. Glaciol. 29 (102), 306–316.
Crockett, A.B., 1998. Background levels of metals in soils, McMurdo Station, Antarctica. Environ. Monit. Assess. 50, 289–296.
Damiani, D., Giorgetti, G., 2008. Provenance of glacial–marine sediments under the McMurdo/Ross Ice Shelf (Windless Bight, Antarctica): heavy minerals and geochemical data. Palaeogeogr. Palaeoclim. 260, 262–283.
de Baar, H.J.W., de Jong, J.T.M., 2001. Distributions, sources and sinks of iron in seawater. In: Turner, D., Hunter, K. (Eds.), The Biogeochemistry of Iron in Seawater. IUPAC Series on Analytical and Physical Chemistry of Environmental Systems, vol. 7. John Wiley & Sons Ltd., Chichester, pp. 123–253.
de Baar, H.J.W., Gerringa, L.J.A., Laan, P., Timmermans, K.R., 2008. Efficiency of carbon removal per added iron in ocean iron fertilization. Mar. Ecol. Progr. Ser. 364, 269–282.
de Jong, J., Schoemann, V., Tison, J.L., Becquevort, S., Masson, F., Lannuzel, D., Petit, J., Chou, L., Weis, D., Mattielli, N., 2007. Precise measurement of Fe isotopes in marine samples by multi-collector inductively coupled plasma mass spectrometry (MC-ICP-MS). Anal. Chim. Acta 589, 105–119.
de Jong, J., Schoemann, V., Lannuzel, D., Tison, J.L., Mattielli, N., 2008. High-accuracy determination of iron in seawater by isotope dilution multiple collector inductively coupled plasma mass spectrometry (ID-MC-ICP-MS) using nitrilotriacetic acid chelating resin for preconcentration and matrix separation. Anal. Chim. Acta 623, 126–139.
de Jong, J., Schoemann, V., Lannuzel, D., Croot, P., de Baar, H., Tison, J.L., 2012. Natural iron fertilization of the Atlantic Southern Ocean by continental shelf sources of the Antarctic Peninsula. J. Geophys. Res. 117, G01029. http://dx.doi.org/10.1029/2011JG001679.
Del Carlo, P., Panter, K.S., Bassett, K., Bracciali, L., Di Vincenzo, G., Rocchi, S., 2009. The upper lithostratigraphic unit of ANDRILL AND-2A core (Southern McMurdo Sound, Antarctica): local Pleistocene volcanic sources, paleoenvironmental implications and subsidence in the southern Victoria Land Basin. Global Planet. Chang. 69, 142–161.

Dinniman, M.S., Klinck, J.M., Smith, W.O., 2007. Influence of sea ice cover and icebergs on circulation and water mass formation in a numerical circulation model of the Ross Sea, Antarctica. J. Geophys. Res. 112 (C11013). http://dx.doi.org/10.1029/2006JC004036.
Domack, E.W., Foss, D.J.P., Syvitski, J.P.M., McClennen, C.E., 1994. Transport of suspended particulate matter in an Antarctic fjord. Mar. Geol. 121, 161–170.
Duce, R.A., Liss, P.S., Merrill, J.T., Atlas, E.L., Buat-Menard, P., Hicks, B.B., et al., 1991. The atmospheric input of trace species to the world ocean. Global Biogeochem. Cy. 5, 193–259.
Dumont, I., Schoemann, V., Lannuzel, D., Chou, L., Tison, J.L., Becquevort, S., 2009. Distribution and characterization of dissolved and particulate organic matter in Antarctic pack ice. Polar Biol. 32, 733–750.
Dunbar, R.B., Leventer, A.R., Stockton, W.L., 1989. Biogenic sedimentation in McMurdo Sound, Antarctica. Mar. Geol. 85, 155–179.
Dunbar, G.B., Bertler, N.A.N., McKay, R.M., 2009. Sediment flux through the McMurdo Ice Shelf in Windless Bight, Antarctica. Global Planet. Chang. 69, 87–93.
Edwards, R., Sedwick, P., 2001. Iron in East Antarctic snow: implications for atmospheric iron deposition and algal production in Antarctic waters. Geophys. Res. Lett. 28, 3907–3910.
Eicken, H., 2003. From the microscopic, to the macroscopic, to the regional scale: growth, microstructure and properties of sea ice. In: Thomas, D.N., Dieckmann, G.S. (Eds.), Sea Ice, an Introduction to its Physics, Chemistry, Biology and Geology. Chichester, Wiley-Blackwell, pp. 22–81.
Ellwood, M.J., Hunter, K.A., 2000. The incorporation of zinc and iron into the frustule of the marine diatom *Thalassiosira pseudonana*. Limnol. Oceanogr. 45, 1517–1524.
Elrod, V.A., Berelson, W.M., Coale, K.H., Johnson, K.S., 2004. The flux of iron from continental shelf sediments: a missing source for global budgets. Geophys. Res. Lett. 31, L12307. http://dx.doi.org/10.1029/2004GL020216.
Epping, E.H.G., Schoemann, V., de Heij, H., 1998. Manganese and iron oxidation during benthic oxygenic photosynthesis. Estuar. Coast Shelf Sci. 47, 753–767.
Fitzwater, S.E., Johnson, K.S., Gordon, R.M., Coale, K.H., Smith, W.O., 2000. Trace metal concentrations in the Ross Sea and their relationship with nutrients and phytoplankton growth. Deep-Sea Res. II 47, 3159–3179.
Garrison, D.L., Sullivan, C.W., Ackley, S.F., 1986. Sea ice microbial communities in Antarctica. BioScience 36, 243–250.
Goffart, A., Catalano, G., Hecq, J.H., 2000. Factors controlling the distribution of diatoms and Phaeocystis in the Ross Sea. J. Mar. Syst. 27, 161–175.
Golden, K.M., Ackley, S.F., Lytle, V.I., 1998. The percolation phase transition in sea ice. Science 282, 2238–2241.
Goring, D.G., Pyne, A., 2003. Observations of sea-level variability in Ross Sea, Antarctica. New Zeal. J. Mar. Fresh 37, 241–249.
Gow, A.J., Ackley, S.F., Govoni, J.W., 1998. Physical and structural properties of land-fast sea ice in McMurdo Sound, Antarctica. Antarct. Res. Ser. 74, 355–374.
Grotti, M., Soggia, F., Abelmoschi, M.L., Rivaro, P., Magi, E., Frache, R., 2001. Temporal distribution of trace metals in Antarctic coastal waters. Mar. Chem. 76, 189–209.
Grotti, M., Soglia, F., Ianni, C., Frache, R., 2005. Trace metals distributions in coastal sea ice of Terra Nova Bay, Ross Sea, Antarctica. Antarct. Sci. 17, 289–300.
Hampel, F.R., 1974. The influence curve and its role in robust estimation. J. Am. Statist. Assoc. 69, 383–393.
Hassler, C., Schoemann, V., 2009. Bioavailability of organically bound Fe to model phytoplankton of the Southern Ocean. Biogeosciences 6, 2281–2296.
Hassler, C.S., Schoemann, V., Mancuso Nichols, C., Butler, E.C.V., Boyd, P.W., 2011. Saccharides enhance iron bioavailability to Southern Ocean phytoplankton. Proc. Natl. Acad. Sci. U. S. A. 108, 1076–1081.
Hieke Merlin, O., Longo Salvador, G., Menegazzo Vitturi, L., Pistolato, M., Rampazzo, G., 1991. Geochemical characteristics of Western Ross Sea (Antarctica) sediments. Mar. Geol. 99, 209–229.
Ikegawa, M., Kimura, M., Honda, K., Makita, K., Fujii, Y., Itokawa, Y., 1997. Springtime peaks of trace metals in Antarctic snow. Environ. Health Perspect. 105 (6), 654–659.
Jeffries, M.O., Weeks, W.F., Shaw, R., Morris, K., 1993. Structural characteristics of congelation and platelet ice and their role in the development of Antarctic land-fast sea ice. J. Glaciol. 39, 223–237.
Johnson, K.S., Boyle, E., Bruland, K., Coale, K., Measures, C., Moffett, J., et al., 2007. Developing standards for dissolved iron in seawater. Eos 88, 131–132.
Kelly, P.J., Kyle, P.R., Dunbar, N.W., Sims, K.W.W., 2008. Geochemistry and mineralogy of the phonolite lava lake, Erebus volcano, Antarctica: 1972–2004 and comparison with older lavas. J. Volcanol. Geoth. Res. 177, 589–605.
Krissek, L.A., Kyle, P.R., 2001. Geochemical indicators of weathering, Cenozoic palaeoclimates, and provenance in fine-grained sediments from CRP-3, Victoria Land Basin, Antarctica. Terra Antarct. 8, 561–568.
Kyle, P.R., 1976. Geology, Mineralogy and Geochemistry of the Late Cenozoic McMurdo Volcanic Group, Victoria Land, Antarctica. PhD thesis Victoria University of Wellington, New Zealand 444.
Kyle, P.R., Meeker, K., Finnegan, D., 1990. Emission rates of sulfur dioxide, trace gases and metals from Mount Erebus, Antarctica. Geophys. Res. Lett. 17, 2125–2128.
Lancaster, N., 2002. Flux of eolian sediment in the McMurdo Dry Valleys, Antarctica: a preliminary assessment. Arct. Antarct. Alp. Res. 34, 318–323.
Lannuzel, D., de Jong, J., Schoemann, V., Trevena, A., Tison, J.L., Chou, L., 2006. Development of a sampling and flow injection analysis technique for iron determination in the sea ice environment. Anal. Chim. Acta 556, 476–483.
Lannuzel, D., Schoemann, V., de Jong, J., Tison, J.L., Chou, L., 2007. Distribution and biogeochemical behaviour of iron in the East Antarctic sea ice. Mar. Chem. 106, 18–32.
Lannuzel, D., Schoemann, V., de Jong, J., Chou, L., Delille, B., Becquevort, S., Tison, J.L., 2008. Iron study during a time series in the western Weddell pack ice. Mar. Chem. 108, 85–95.
Lannuzel, D., Schoemann, V., de Jong, J., Pasquer, B., van der Merwe, P., Masson, F., Tison, J.L., Bowie, A., 2010. Distribution of dissolved iron in Antarctic sea ice: spatial, seasonal, and inter-annual variability. J. Geophys. Res. 115, G03022. http://dx.doi.org/10.1029/2009JG001031.
Legendre, L., Ackley, S.F., Dieckmann, G.S., Gulliksen, B., Horner, R., Hoshiai, T., Melnikov, I.A., Reeburgh, W.S., Spindler, M., Sullivan, C.W., 1992. Ecology of sea ice biota. 2. Global significance. Polar Biol. 12, 429–444.
Leonard, G.H., Purdie, C.R., Langhorne, P.J., Haskell, T.G., Williams, M.J.M., Frew, R.D., 2006. Observations of platelet ice growth and oceanographic conditions during the winter of 2003 in McMurdo Sound, Antarctica. J. Geophys. Res. 111, C04012. http://dx.doi.org/10.1029/2005JC002952.
Leventer, A., Dunbar, R.B., 1987. Diatom flux in McMurdo Sound, Antarctica. Mar. Micropaleontol. 12, 49–64.
Löscher, B.M., de Baar, H.J.W., de Jong, J.T.M., Veth, C., Dehairs, F., 1997. The distribution of Fe in the Antarctic Circumpolar Current. Deep-Sea Res. II 44, 143–188.
Mahaney, W.C., Dohm, J., Kapran, B., Hancock, R.G.V., Milner, M.W., 2009. Secondary Fe and Al in Antarctic paleosols: correlation to Mars with prospect for the presence of life. Icarus 203, 320–330.
Mahoney, A.M., Gough, A.J., Langhorne, P.J., Robinson, N.J., Stevens, C.L., Williams, M.J.M., Haskell, T.G., 2011. The seasonal arrival of ice shelf water in coastal Antarctica and its effect on sea ice growth. J. Geophys. Res. 116, C11032. http://dx.doi.org/10.1029/2011JC007060.
Martin, J.H., Knauer, G.A., 1973. The elemental composition of plankton. Geochim. Cosmochim. Acta 37, l639–l1653.
Mazzera, D.M., Lowenthal, D.H., Chow, J.C., Watson, J.G., Grubisic, V., 2001. PM10 measurements at McMurdo Station, Antarctica. Atmos. Environ. 35, 1891–1902.
McConnell, J.R., Aristarain, A.J., Banta, J.R., Edwards, P.R., Simoes, J.C., 2007. 20th-century doubling in dust archived in an Antarctic Peninsula ice core parallels climate change and desertification in South America. Proc. Natl. Acad. Sci. U. S. A. 104, 5743–5748.
Nicol, S., Bowie, A., Jarman, S., Lannuzel, D., Meiners, K.M., van der Merwe, P., 2010. Southern Ocean iron fertilization by baleen whales and Antarctic krill. Fish Fish 11 (2), 203–209.
Pakhomova, S.V., Hall, P.O.J., Kononets, M.I., Rozanov, A.G., Tengberg, A., Vershinin, A.V., 2007. Fluxes of iron and manganese across the sediment–water interface under various redox conditions. Mar. Chem. 107, 319–331.
Planquette, H., Statham, P.J., Fones, G.R., Charette, M.A., Moore, C.M., Salter, I., Nédélec, F.H., Taylor, S.L., French, M., Baker, A.R., Mahowald, N., Jickells, T.D., 2007. Dissolved iron in the vicinity of the Crozet Islands, Southern Ocean. Deep-Sea Res. II 54, 1999–2019.
Planquette, H., Fones, G.R., Statham, P.J., Morris, P.J., 2009. Origin of iron and aluminium in large particles (<53 μm) in the Crozet region, Southern Ocean. Mar. Chem. 115, 31–42.
Purdie, C., Langhorne, P., Leonard, G., Haskell, T., 2006. Growth of first year land-fast Antarctic sea ice determined from winter temperature measurements. Ann. Glaciol. 44, 170–176.
Rémy, J.P., 2005. Caractérisation du réseau microbien de la glace de mer côtière du détroit de McMurdo (Antarctique). Master thesis Université Libre de Bruxelles, Belgium.
Rémy, J.P., Becquevort, S., Haskell, T.G., Tison, J.L., 2008. Impact of the B-15 iceberg stranding event on the physical and biological properties of sea ice in McMurdo Sound, Ross Sea, Antarctica. Antarct. Sci. http://dx.doi.org/10.1017/S0954102008001284.
Rivaro, P., Ianni, C., Massolo, S., Abelmoschi, M.L., De Vittor, C., Frache, R., 2011. Distribution of dissolved labile and particulate iron and copper in Terra Nova Bay polynya (Ross Sea, Antarctica) surface waters in relation to nutrients and phytoplankton growth. Cont. Shelf Res. 31, 879–889.
Rivaro, P., Abelmoschi, M.L., Grotti, M., Ianni, C., Magi, E., Margiotta, F., Massolo, S., Saggiomo, V., 2012. Combined effects of hydrographic structure and iron and copper availability on the phytoplankton growth in Terra Nova Bay Polynya (Ross Sea, Antarctica). Deep-Sea Res. I 62, 97–110.
Robinson, N.J., 2004. An Oceanographic Study of the Cavity Beneath the McMurdo Ice Shelf, Antarctica. Master thesis Victoria University of Wellington, New Zealand 146.
Robinson, N.J., Williams, M.J.M., Barrett, P.J., Pyne, A.R., 2010. Observations of flow and ice–ocean interaction beneath the McMurdo Ice Shelf, Antarctica. J. Geophys. Res. 115, C03025. http://dx.doi.org/10.1029/2008JC005255.
Sarthou, G., Timmermans, K.R., Blain, S., Tréguer, P., 2005. Growth physiology and fate of diatoms in the ocean: a review. J. Sea Res. 53, 25–42.
Sarthou, G., Vincent, D., Christaki, U., Obernosterer, I., Timmermans, K.R., Brussaard, C.P.D., 2008. The fate of biogenic iron during a phytoplankton bloom induced by natural fertilisation: impact of copepod grazing. Deep-Sea Res. II 55, 734–751.
Schmidt, K., Atkinson, A., Steigenberger, S., Fielding, S., Lindsay, M.C.M., Pond, D.W., Tarling, G.A., Klevjer, T.A., Allen, C.S., Nicol, S., Achterberg, E.P., 2011. Seabed foraging by Antarctic krill: implications for stock assessment, bentho-pelagic coupling, and the vertical transfer of iron. Limnol. Oceanogr. 56 (4), 1411–1428.
Sedwick, P.N., DiTullio, G.R., 1997. Regulation of algal blooms in Antarctic shelf waters by the release of iron from melting sea ice. Geophys. Res. Lett. 24, 2515–2518.
Sedwick, P.N., DiTullio, G.R., Mackey, D.J., 2000. Iron and manganese in the Ross Sea, Antarctica: seasonal iron limitation in Antarctic shelf waters. J. Geophys. Res. 105 (C5), 11321–11336.
Sedwick, P.N., Marsay, C.M., Sohst, B.M., Aguilar-Islas, A.M., Lohan, M.C., Long, M.C., Arrigo, K.R., Dunbar, R.B., Saito, M.A., Smith, W.O., DiTullio, G.R., 2011. Early season depletion of dissolved iron in the Ross Sea polynya: implications for iron dynamics on the Antarctic continental shelf. J. Geophys. Res. 116, C12019. http://dx.doi.org/10.1029/2010JC006553.
Severmann, S., McManus, J., Berelson, W.M., Hammond, D.E., 2010. The continental shelf benthic iron flux and its isotopic composition. Geochim. Cosmochim. Acta. 74, 3984–4004.
Shemesh, A., Mortlock, R.A., Smith, R.J., Froelich, P.N., 1988. Determination of Ge/Si in marine siliceous microfossils: separation, cleaning and dissolution of diatoms and radiolaria. Mar. Chem. 25, 305–323.
Sleewaegen, S., Lorrain, R., Offer, Z., Azmon, E., Fitzsimons, S., Souchez, R., 2002. Trapping of aeolian sediments and build-up of the ice cover of a dry-based Antarctic lake. Earth Surf. Process. Landforms 27, 307–315.

Smedsrud, L.H., Jenkins, A., 2004. Frazil ice formation in an ice shelf water plume. J. Geophys. Res. 109, C03025. http://dx.doi.org/10.1029/2003JC001851.
Smith, I.J., Langhorne, P.J., Haskell, T.G., Trodahl, H.J., Frew, R., Vennell, M.R., 2001. Platelet ice and the land-fast sea ice of McMurdo Sound, Antarctica. Ann. Glaciol. 33, 21–27.
Sunda, W., 2001. Bioavailability and bioaccumulation of iron in the sea. In: Turner, D., Hunter, K. (Eds.), The Biogeochemistry of Iron in Seawater. IUPAC Series on Analytical and Physical Chemistry of Environmental Systems, vol. 7. John Wiley & Sons Ltd., Chichester, pp. 41–84.
Tovar-Sanchez, A., Duarte, C.M., Hernandez-Leon, S., Sanudo-Wilhelmy, S.A., 2007. Krill as a central node for iron cycling in the Southern Ocean. Geophys. Res. Lett. 34 (11), L11601. http://dx.doi.org/10.1029/2006GL029096.
Trodahl, H.J., McGuinness, M., Langhorne, P.J., Collins, K., Pantoja, A.E., Smith, I.J., Haskell, T.G., 2000. Heat transport in McMurdo Sound first year fast ice. J. Geophys. Res. 105 (C5), 11347–11358.
van der Merwe, P., Lannuzel, D., Mancuso Nichols, C.A., Meiners, K., Heil, P., Norman, L., Thomas, D.N., Bowie, A.R., 2009. Biogeochemical observations during the winter–spring transition in East Antarctic sea ice: evidence of iron and exopolysaccharide controls. Mar. Chem. 115, 163–175.
van der Merwe, P., Lannuzel, D., Bowie, A.R., Mancuso Nichols, C.A., Meiners, K.M., 2011a. Iron fractionation in pack and fast ice in East Antarctica: temporal decoupling between the release of dissolved and particulate iron during spring melt. Deep-Sea Res. I 58, 1222–1236.
van der Merwe, P., Lannuzel, D., Bowie, A.R., Meiners, K.M., 2011b. High temporal resolution observations of spring fast-ice melt and seawater iron enrichment in East Antarctica. J. Geophys. Res. 116, G03017. http://dx.doi.org/10.1029/2010JG001628.
van Lipzig, N.P.M., King, J.C., Lachlan-Cope, T.A., van den Broeke, M.R., 2004. Precipitation, sublimation, and snow drift in the Antarctic Peninsula region from a regional atmospheric model. J. Geophys. Res. 109, D24106. http://dx.doi.org/10.1029/2004JD004701.
Wagener, T., Guieu, C., Losno, R., Bonnet, S., Mahowald, N., 2008. Revisiting atmospheric dust export to the Southern Hemisphere ocean: biogeochemical implications. Global Biogeochem Cy 22, GB2006. http://dx.doi.org/10.1029/2007GB002984.
Westerlund, S., Öhman, P., 1991. Iron in the water column of the Weddell Sea. Mar. Chem. 35, 199–217.
Williamson, B.R., Kreutz, K.J., Mayewski, P.A., Bertler, N.A.N., Sneed, S., Handley, M., Introne, D., 2007. A coastal transect of McMurdo Dry Valleys (Antarctica) snow and firn: marine and terrestrial influences on glaciochemistry. J. Glaciol. 53, 681–693.